PHILOSOPHICAL TRANSACTIONS OF THE ROYAL SOCIETY A
MATHEMATICAL, PHYSICAL & ENGINEERING SCIENCES

# Crack Problems in a Poroelastic Medium: An Asymptotic Approach

R. V. Craster and C. Atkinson

*Phil. Trans. R. Soc. Lond. A* 1994 **346**, 387-428
doi: 10.1098/rsta.1994.0026

# Crack problems in a poroelastic medium: an asymptotic approach

BY R. V. CRASTER[1] AND C. ATKINSON[2]

[1] *Department of Applied Mathematics and Theoretical Physics, University of Cambridge, Cambridge CB3 9EW, U.K.*

[2] *Department of Mathematics, Imperial College of Science, Technology and Medicine, London SW7 2BZ, U.K*

## Contents



We consider problems involving semi-infinite cracks in a porous elastic material. The cracks are loaded with a time dependent internal stress, or pore pressure. Either mixed or unmixed pore pressure boundary conditions on the fracture plane are considered. An asymptotic procedure that partly uncouples the elastic and fluid responses is used, allowing an asymptotic expression for the stress intensity factors as time progresses to be obtained. The method allows the physical processes involved at the crack tip and their interactions to be studied. This is an advance on previous methods where results were obtained in Laplace transform space and inverted numerically to obtain real-time solutions.

The crack problems are formulated using distributions of dislocations (and pore pressure gradient discontinuities when necessary) to generate integral equations of the Wiener–Hopf type. The resulting functional equations are, of course, identical to those considered by C. Atkinson and R. V. Craster, but with the alternative formulation we develop an asymptotic procedure which should be ap-

*Phil. Trans. R. Soc. Lond.* A (1994) **346**, 387–428

*Printed in Great Britain*

plicable to other problems (e.g. finite length cracks). This asymptotic procedure can be used to derive asymptotic expansions for more complicated loadings when the numerical effort involved in evaluating results would be excessive.

A large-time asymptotic method is also briefly described which complements the small-time method.

The operators for poroelastic crack problems are inverted for a particular loading; the reciprocal theorem for poroelasticity is used together with eigensolutions of the fundamental problems to deduce the stress (or where necessary the pore pressure gradient) intensity factors for any loading. These formulae extend previous results allowing a wide range of different loadings to be considered. As an example, the stress intensity factor for a point loaded crack is derived and the asymptotic method is applied to this problem to derive a simple asymptotic formula.

Finally, an invariant integral, which is a generalization of the Eshelby energy-momentum tensor, is used to derive integral identities which serve as a check on the intensity factors in some situations.

## 0. Nomenclature

| | |
|---|---|
| $\alpha$ | Biot's coefficient of effective stress, i.e. the ratio of fluid volume to the volume change of solid allowing the fluid to drain, where $0 < \alpha \leqslant 1$ |
| $B$ | Skempton's pore pressure coefficient (Skempton 1954), i.e. the ratio of induced pore pressure to the variation of mean normal compression under undrained conditions |
| $c$ | generalized consolidation coefficient |
| $\delta_{ij}$ | Kronecker delta |
| $e$ | dilatation |
| $\epsilon_{ij}$ | components of the strain tensor, $e = \epsilon_{kk}$ |
| $\kappa$ | permeability coefficient |
| $G$ | the shear modulus |
| $\mathrm{d}\zeta/\mathrm{d}p\vert_{\epsilon}$ | a measure of the change in fluid content generated in a unit reference volume during a change of pressure with the strains kept constant$(= Q^{-1})$ |
| $m$ | mass of fluid per unit volume |
| $\nu, \nu_{\mathrm{u}}$ | drained and undrained Poisson ratios, where $\nu \leqslant \nu_{\mathrm{u}} \leqslant 0.5$ |
| $p$ | perturbation pore pressure, i.e. the increase in fluid pressure from a reference pressure $p_0$ |
| $q_i$ | mass flux vector |
| $\rho_0$ | reference density |
| $\sigma_{ij}$ | stress tensor |
| $u_i$ | displacement vector |
| $\zeta$ | variation of fluid content per unit reference volume, i.e. mass of fluid per unit volume/initial density $\rho_0$ (thus $m = \rho_0\zeta$) |





PHILOSOPHICAL TRANSACTIONS OF THE ROYAL SOCIETY A MATHEMATICAL, PHYSICAL & ENGINEERING SCIENCES

The following relations are used in the text.

$$\alpha = \frac{3(\nu_u - \nu)}{B(1-2\nu)(1+\nu_u)}, \quad Q = \frac{2GB^2(1-2\nu)(1+\nu_u)^2}{9(\nu_u-\nu)(1-2\nu_u)},$$

$$\eta = \frac{1-\nu}{1-2\nu}, \quad \overline{\eta} = \frac{(1-\nu)}{2(\nu_u - \nu)},$$

$$2G_u = \frac{2GB(1+\nu_u)}{3(1-\nu_u)}, \quad c = \frac{2\kappa B^2 G(1-\nu)(1+\nu_u)^2}{9(1-\nu_u)(\nu_u-\nu)},$$

$$N_0 = \tfrac{1}{2}(1-2\overline{\eta}).$$

## 1. Introduction

The equations of linear, isotropic poroelasticity were introduced by Biot (1941) and were shown to be mathematically equivalent to the fully coupled thermoelastic equations by Biot (1955). Hence, the results below are valid for fully coupled thermoelastic materials. For thermoelastic materials a coupling parameter appears which is typically small, this is usually used to uncouple the equations, leading to the theory of thermal stresses. For a poroelastic material the equations are fully coupled and no such approximation can be made, hence we refer primarily to poroelastic variables in the following. Noting the mathematical analogy between temperature and pore pressure, fluid volume content and entropy the results can be interpreted in terms of thermoelastic variables if necessary.

The poroelastic theory attempts to model the mechanical response of a porous material which has a solid elastic skeleton with the pore space filled with a viscous fluid. The equations derived by Biot involve a coupling of the theories of elasticity and diffusion; there is an explicit coupling between the dilatation of the elastic skeleton and the pressure in the diffusing pore fluid. The governing equations can be derived by using Darcy's equation to model the diffusion process, a mass conservation equation for the pore fluid and the equilibrium equation for the stress. The equations were derived by Biot using this phenomenological approach and have subsequently been derived using homogenization theory (Auriault 1980; Burridge & Keller 1981) and mixture theory (Bowen 1982). Hence, the fundamental basis of the equations is well founded. The poroelastic materials differ from the corresponding quasi-static elastic solids as a time dependence is introduced into the otherwise time independent elasticity equations. This diffusing pore fluid can have a large effect; for example, for rapid loadings (compared with the diffusion timescale) the material response is stiffer than for slower loadings as the fluid has less time to diffuse away. In particular the stress intensity factors which characterize the singular near crack tip stress fields for fracture problems are time dependent, and depend upon the pore pressure boundary conditions on the fracture plane.

The theory is relevant to the fracture of rocks and can be applied to geophysical problems (for a review, see Rudnicki 1985). This work is motivated by applications to fracture and fault initiation, propagation and creep in porous rocks. Such problems of fracture where there is pore fluid interaction are believed to be important in fault creep and in enhancing the recovery of oil via the hydraulic fracturing process. The sequence of model problems considered here is aimed at





PHILOSOPHICAL TRANSACTIONS OF THE ROYAL SOCIETY A MATHEMATICAL, PHYSICAL & ENGINEERING SCIENCES

understanding and modelling the physical processes that occur. As an example, one can imagine that during the initiation of fracture in the hydraulic fracturing process, when a crack is pressurized by pumping fluid into it, the fluid in the crack may leak out into the formation. This causes a volume expansion of the material around the crack, tending to close the fracture. There will also be external stress or pore pressure fields which may affect the fracture. Therefore, there is a complicated interaction between the diffusing pore fluid and applied loading, which must be modelled correctly if fracture in fluid filled materials is to be understood.

The equations taken here are quasi-static, the effect of inertia is neglected; this is because the effects which we are considering should happen on a timescale large compared with that for wave propagation. It should be noted that Biot extended his theory to include inertia (see, for example, Biot 1956 *a*, *b*) and that some attempts at solving the fully coupled dynamic thermoelastic crack problems are possible (Atkinson & Craster 1992*b*).

The governing equations used are those of Biot (1941), which were reformulated by Rice & Cleary (1976, hereafter [RC]). The equations are characterized by five independent constants; $G$, $\nu$, $\nu_u$, $\kappa$ and $B$ (the shear modulus, drained and undrained Poisson's ratios, the permeability coefficient and Skempton's pore pressure coefficient) some typical values of these parameters are given in [RC]. For instance values given there (for Berea sandstone) are $\nu_u = 0.33$, $\nu = 0.2$, $B = 0.62$, $G = 60$ kbar, $c$ (for water saturated sandstone)$= 1.6 \times 10^4$ cm s$^{-2}$, (for Westerly Granite) are $\nu_u = 0.34$, $\nu = 0.25$, $B = 0.85$, $G = 150$ kbar, $c$ (for water saturated) $= 0.22$ cm s$^{-2}$ the material properties of rocks vary widely, particularly in their permeabilities. The theory is also applicable to saturated clays, this soil mechanics limit is recovered by taking $\nu_u \to \frac{1}{2}$, $B \to 1$ with the results that in the notation used here (see Nomenclature) $G_u \to G$, $\overline{\eta} \to \eta$, $\alpha \to 1$, $c \to 2G\eta\kappa$ and $Q \to \infty$. The pore space can, of course, be filled with more viscous fluids, hence it is advantageous to keep the theory as general as possible.

The stress $\sigma_{ij}$ is given by

$$\sigma_{ij} = 2G\epsilon_{ij} + \frac{2G\nu}{(1-2\nu)}\delta_{ij}e - \alpha p\delta_{ij}, \tag{1.1}$$

with $\epsilon_{ij}$ as the strain tensor and $e = \epsilon_{kk}$ is the dilatation. The pore pressure, $p$, satisfies the following relation between the variation of fluid volume content, $\zeta$, and the dilatation, $e$,

$$p = Q\zeta - \alpha Qe. \tag{1.2}$$

Provided there are no body forces or fluid sources the governing equations can be written as the equilibrium equation for the stresses

$$\sigma_{ij,j} = 0, \tag{1.3}$$

Darcy's law which relates the mass flux to the gradient of the pore pressure,

$$q_i = -\rho_0\kappa p_{,i}, \tag{1.4}$$

and a mass conservation equation for the fluid

$$\partial m/\partial t = -q_{i,i}, \tag{1.5}$$

with $m$ the mass of fluid per unit volume and $\rho_0$ as the reference density. The





PHILOSOPHICAL TRANSACTIONS OF THE ROYAL SOCIETY A MATHEMATICAL, PHYSICAL & ENGINEERING SCIENCES

equations can be written as an elastic Navier equation with a coupling term for the pore pressure and as a diffusion equation for the pore pressure with a coupling term for the dilatation, i.e.

$$G\nabla^2 u_i + \frac{G}{(1-2\nu)} e_{,i} - \alpha p_{,i} = 0, \quad \frac{\partial p}{\partial t} - \kappa Q \nabla^2 p = -\alpha Q \frac{\partial e}{\partial t}. \tag{1.6}$$

In our previous papers (Atkinson & Craster 1991; Craster & Atkinson 1992*a*; hereafter [AC] and [CA]) on time-dependent fracture in a poroelastic material, the governing equations have been solved for an impulsively applied and spatially exponentially decaying internal stress or pore pressure loading on the crack faces of a semi-infinite crack. Solutions for the time-dependent stress intensity factors were found using the Wiener–Hopf technique after the governing equations had been Fourier transformed in space and Laplace transformed in time. In more complicated cases, those with mixed boundary conditions for the pore pressure on the fracture plane, a matrix functional equation was solved. Fortunately, this matrix could be solved by first solving a subsidiary equation. The stress intensity factors and the coefficients of the singular pore pressure gradient as functions of the Laplace transform parameter were found; these transforms were then inverted numerically. It is the aim of this paper to analyse and extend these results further, by formulating the problems in an alternative manner which will make it simpler to understand the processes at work. In particular we evaluate the Laplace transforms as an asymptotic expansion in time and attempt to interpret the physical mechanisms which are driving time dependent terms in the stress intensity factors. In doing so we avoid inverting Laplace transforms numerically; this can be a difficult, and time consuming, numerical process, especially if the Laplace transform parameter is embedded in a complicated formula, i.e. the stress intensity factor in (4.15). We have used both the Stehfest (1970) and Talbot (1979) algorithms, preferring (in hindsight) the latter. For a review of numerical methods for Laplace transform inversion see Davies & Martin (1979) and a bibliography, Piessens (1975).

The plan of the paper is as follows. First, we consider one of the simpler cases which has unmixed pore pressure boundary conditions along the fracture plane. Specifically, a semi-infinite permeable crack subjected to a spatially exponentially decaying, impulsively applied, shear loading. An asymptotic procedure for solving the problem is developed and an asymptotic expansion for the stress intensity factor in real time is given. The functional equations for the example case are derived from a distribution of dislocations. Dislocation solutions are derived here from the potential representations for the poroelastic equations given in Craster & Atkinson (1992*b*) together with the transform inverses in Appendix A. These dislocation solutions are well known ([RC]; Rudnicki 1987) and could alternatively be evaluated using the complex variable technique as outlined in [RC]. The dislocations have the useful property that they can be interpreted as being the sum of an elastic dislocation (for an undrained material) and a pore fluid dipole which is orientated to maintain the pore pressure boundary condition. Although crack problems cannot be similarly uncoupled, it is possible to use the property that poroelastic displacement dislocations separate into elastic and fluid driven components to identify the asymptotic sequence of events in real time. For the unmixed case (i.e. the pore pressure boundary condition is unmixed on the fracture plane) we formulate the problem as an integral equation for the stress in terms of an unknown dislocation density. This equation is of Wiener–Hopf type; we proceed to solve this problem using an asymptotic method for small times relative to the diffusional timescale, thereby evaluating the 'outer' field and the near crack tip field as they develop. The procedure is first to approximate the Wiener–Hopf kernel in the limit of small times in an 'outer' limit and to correct for any errors by rescaling the equations in an 'inner' limit. This method is similar in principle to that developed by Atkinson (1975) for elastic cracks interacting with boundaries.

The asymptotic method is also applied to more complicated mixed problems (i.e. the pore pressure boundary conditions are different on the crack faces from those on the fracture plane ahead of the crack) where we now have two coupled integral equations to solve. We have integral equations for the stress and pore pressure in terms of unknown distributions of dislocations and pore pressure gradient (or pore pressure) discontinuities, these are treated in a similar manner.

The results for the intensity factors, as defined in (1.9) and (1.10) below, are checked using an invariant integral based on a 'pseudo' energy momentum tensor (Atkinson & Smelser 1982), which is a generalization of the Eshelby (1951) energy momentum tensor. These checks lead to two integral identities which have to be verified numerically and demonstrate the power of invariant integrals to check complicated results in a relatively straightforward fashion.

The reciprocal theorem is applied to the crack problems to give formulae for the stress (and pore pressure) intensity factors for any applied loading. Eigensolutions of the crack problems are generated from the functional equations; these combine with the known asymptotic behaviour of the 'real' crack problem to isolate the intensity factors in terms of a single line integral. As an example of the asymptotic method developed here, the method is applied to the problem of a point loaded crack to derive a simple asymptotic formula for this loading.

The transform inverses and necessary results from previous papers to make this paper self contained are given in the Appendices.

In the following we work extensively in Fourier transform space, defining the Fourier transform of $\phi(X)$ as

$$\overline{\phi}(\xi) = \int_{-\infty}^{\infty} \phi(X) \mathrm{e}^{\mathrm{i}\xi X}\, \mathrm{d}X. \tag{1.7}$$

We use $\xi$ as the Fourier transform variable and also half-range transforms, i.e.

$$\overline{\psi}_{+}(\xi) = \int_{0}^{\infty} \psi(X) \mathrm{e}^{\mathrm{i}\xi X}\, \mathrm{d}X, \tag{1.8}$$

the subscript $+$ denotes that the transform is analytic in the upper half of the complex $\xi$ plane. A 'minus' transform is similarly defined as the integral from $-\infty$ to 0 and is analytic in the lower half plane. The functions $|\xi|$ and $\Gamma = (\xi^2+1)^{1/2}$ used in the text are defined to be that branch of the square root with positive real part and can be factorized into the products of functions analytic in the upper and lower complex $\xi$ planes respectively. The function $|\xi| = \xi_{+}^{1/2}\xi_{-}^{1/2}$ and has branch cuts from $\mathrm{i}0_{\pm}$ to $\pm\mathrm{i}\infty$. These branch cuts at the origin can be formally considered to be at $\pm\mathrm{i}d$ where $d$ tends to zero. The function $\Gamma$ is defined as $\Gamma = \Gamma_{+}\Gamma_{-}$, where $\Gamma_{\pm} = (\xi \pm \mathrm{i})^{1/2}$ with branch cuts from $\mp\mathrm{i}$ to $\mp\mathrm{i}\infty$ respectively.

In the limit as $r \to 0$ ($r$ is the radial distance from the crack tip and $\theta$ the polar angle, with $\theta = 0$ the fracture plane ahead of the crack tip) the asymptotic behaviour of the stresses and pore pressure can be determined, i.e. for the tensile stress loaded, mixed problem, the asymptotic behaviour is given from [AC] by

$$p(r,\theta,t) \sim K_2(t)(r/2\pi)^{1/2}\cos(\tfrac{1}{2}\theta), \tag{1.9}$$

$$\sigma_{ij}(r,\theta,t) \sim \frac{K_1(t)}{(2\pi r)^{1/2}} f_{ij}(\theta), \tag{1.10}$$

where $f_{ij}(\theta)$ is the usual elastic angular dependence. The functions $K_1(t), K_2(t)$ are the mode 1 stress intensity and the pore pressure gradient intensity factors respectively. The intensity factors quantify the dominant near crack tip $\delta$ fields; it is the aim of this work to evaluate these intensity factors and determine how they are generated by the elastic-diffusion process.

For antisymmetric loadings, we use $K_3(t)$ to denote the pore pressure gradient intensity factor and $K_{\rm II}(t)$ to denote the mode 2 stress intensity factor, see Appendix D.

In cases which are unmixed in the pore pressure boundary condition on the fracture plane the pore pressure gradient is not singular at the crack tip. The pore pressure gradient intensity factors are zero in these cases and only stress intensity factors need to be identified.

## 2. The semi-infinite permeable crack

As an example of the asymptotic method we present it by using the method on one of the problems treated in [CA]. Let us consider a permeable crack in a poroelastic medium which is in equilibrium for $t < 0$ and is impulsively loaded, at $t = 0$, with an internal shear load. In this case the boundary conditions for the equivalent half-plane problem, on $y = 0$, are

$$p(x,y,t) = 0, \quad \sigma_{22}(x,y,t) = 0 \text{ for all } x, \tag{2.1}$$

$$u_1(x,y,t) = 0, x > 0, \quad \sigma_{12}(x,y,t) = \tau_0 \mathrm{e}^{x/a} H(t) \text{ for } x < 0. \tag{2.2}$$

This is one of the simpler cases, as the pore pressure boundary condition is not mixed on the fracture plane, so a scalar functional equation is obtained (a mixed case would be an impermeable crack, the antisymmetric loading implies a $p = 0$ boundary condition on the fracture plane ahead of the crack tip; this leads to a matrix problem which is treated in [CA]). The crack problem given by (2.1) and (2.2) reduces to the following scalar Wiener–Hopf equation in Fourier and Laplace transform space

$$\frac{\tau_+}{N_+\xi_+^{1/2}} - \frac{\tau_0 c^{1/2} a_1}{s^{3/2}(1+\mathrm{i}\xi a_1)}\left(\frac{1}{N_+\xi_+^{1/2}} - \frac{1}{N_+(\mathrm{i}/a_1)(\mathrm{i}/a_1)_+^{1/2}}\right)$$

$$= -\frac{(2G_{\rm u})^2\kappa}{c} U_- N_- \xi_-^{1/2} + \frac{\tau_0 c^{1/2} a_1}{s^{3/2}(1+\mathrm{i}\xi a_1) N_+(\mathrm{i}/a_1)(\mathrm{i}/a_1)_+^{1/2}} = \Sigma(\xi). \tag{2.3}$$

The derivation from potential representations of the governing equations is given in [CA]. Briefly, the governing equations are Laplace transformed in time ($s$ is the Laplace transform variable) and then scaled to isolate $s$ in the non-dimensional variable $a_1 = a(s/c)^{1/2}$ or as $s^{3/2}$ in the loading term. Fourier transforming with respect to the $X$ variable, ($\xi$ being the Fourier transform variable with respect to the scaled $x$ coordinate $X = x(s/c)^{1/2}$) then reduces the governing equations to a system of differential equations depending only on $Y$. The functions $\tau_+, U_-$ are half range Fourier transforms of the shear stress and displacement (on $y = 0$) respectively.

The function $N(\xi)$ occurs naturally due to the interaction of the permeable boundary conditions on the crack and applied loading; it is given as

$$N(\xi) = \xi^2 - |\xi|(\xi^2+1)^{1/2} + \overline{\eta}. \tag{2.4}$$

This is split into a product of functions analytic in appropriate half planes in [AC] and in a form more amenable to asymptotic analysis in Appendix A of this paper. Using Liouville's theorem and appropriate edge conditions (the pore pressure is non-singular and the displacements are finite) at the crack tip, the entire function $\Sigma(\xi)$ is deduced to be identically zero. Using results from the functional equation all the quantities of interest can be deduced, i.e. the transformed pore pressure is deduced as

$$\frac{3P(\xi,Y,s)}{2B(1+\nu_{\mathrm{u}})} = \frac{\mathrm{i}\overline{\eta}\xi_-^{1/2}(\mathrm{e}^{-|\xi|Y} - \mathrm{e}^{-\Gamma Y})}{N_-}\left(\frac{\tau_0 c^{1/2} a_1}{s^{3/2}(1+\mathrm{i}\xi a_1)N_+(\mathrm{i}/a_1)(\mathrm{i}/a_1)_+^{1/2}}\right). \tag{2.5}$$

This consists of a diffusional part (the $\mathrm{e}^{-\Gamma Y}$ term) and a dilatational response (the $\mathrm{e}^{-|\xi|Y}$ term) which maintains the pore pressure boundary condition on the fracture plane. The stress intensity factor (in the transform variable $s$) is deduced from (2.3) to be

$$\overline{K}_{\mathrm{II}}(s) = \sqrt{2}a^{1/2}\tau_0/sN_+(\mathrm{i}/a_1). \tag{2.6}$$

We recall that the $s$ dependence is contained in $a_1$ which is defined as $a_1 = a(s/c)^{1/2}$. In the limit of small times (equivalently in Laplace transform space as $s \to \infty$) this result can be checked independently using an energy release rate argument as discussed in [CA]. By using the asymptotic expression for $N_+(\xi)$ derived in Appendix A for $\xi$ small, we deduce that

$$\begin{aligned} K_{\mathrm{II}}(t') = \frac{\sqrt{2}\,a^{1/2}\tau_0}{N_+(0)}\Bigg(&H(t') + \frac{1}{\pi\overline{\eta}}(t'/\pi)^{1/2}\left(4 - \gamma - \log t' - \frac{2\overline{\eta}h}{(\frac{1}{2}\overline{\eta})^{1/2}N_+(0)}\right) \\ &+\frac{t'}{\pi^2\overline{\eta}^2}\left(\frac{1}{2} - \frac{\overline{\eta}h}{(\frac{1}{2}\overline{\eta})^{1/2}N_+(0)} + \frac{\overline{\eta}}{N_+^2(0)}(h^2+\tfrac{1}{2}\pi^2)\right. \\ &+\frac{1}{2}\left(1 - \frac{\overline{\eta}h}{(\frac{1}{2}\overline{\eta})^{1/2}N_+(0)}\right)(1-\gamma-\log(t'/4)) \\ &\left. + \tfrac{1}{8}((1-\gamma-\log(t'/4))^2 + 1 - \tfrac{1}{6}\pi^2)\right) + O(t'^{3/2})\Bigg), \end{aligned} \tag{2.7}$$

for small times, where $h = \operatorname{arccot}[(\frac{1}{2}\overline{\eta}N_+^2(0) - 1)^{1/2}]$. In (2.7) $\gamma$ is Euler's constant and the Laplace transform results required are given in Appendix A. A graph of this asymptotic form of the stress intensity factor (which is normalized by dividing through by $\sqrt{2}\tau_0 a^{1/2}$) as a function of the non-dimensionalized timescale $t' = tc/a^2$ (for $\nu = 0.3$, $\nu_{\mathrm{u}} = 0.4$) is shown in figure 1.

Also shown there for comparison is the full solution for the stress intensity

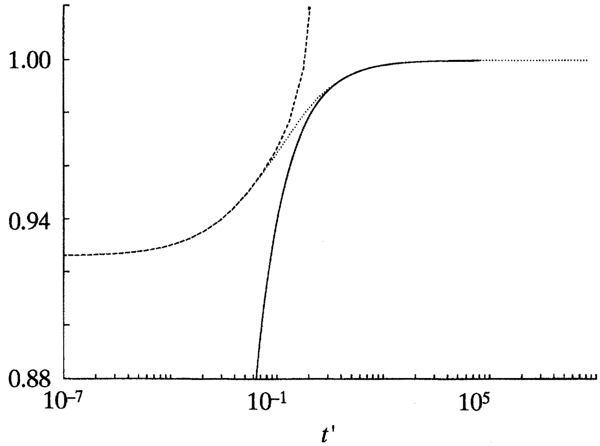


Figure 1. The non-dimensionalized mode 2 stress intensity factor (for $\nu = 0.3, \nu_{\mathrm{u}} = 0.4$) against time, for the full solution, dotted line, the small time solution, dashed line, and the large time solution, solid line.

factor which is inverted numerically using the Talbot (1979) algorithm. From figure 1, the asymptotic result is extremely accurate for small values of the non-dimensional timescale $t'$; this requires minimal computational effort, whereas a numerical method can be time consuming. For some materials where the consolidation parameter is small the asymptotic solution would be valid over a relatively long period of time and hence is effectively the whole solution in these cases. This solution is of value as it gives a real time result for the stress intensity factor. It is also interesting as we hope the analysis of the integral equations will help us to understand which terms in this expansion are driven by different physical processes.

The pore pressure result (2.5) can also be checked independently in the neighbourhood of the crack tip by using the asymptotic result for the pore pressure deduced by an eigenvalue argument in [CA]. The solution above gives the full solution for all the variables of interest, here we want to test the matching procedure for this example as we have this exact solution for comparison.

### (*a*) *An integral equation method*

In this section we outline how a simple asymptotic method can be applied to deduce the solution, for small times, for the above example. We aim to show the method we want to use for more complicated problems works correctly for the semi-infinite model problem, and to try to understand the physical processes which drive the stress intensity factor for small times. In the following analysis we use the Laplace transform in time, with $s$ the Laplace transform parameter. From the dislocation solutions given in Appendix C, the stress on the $x$ axis is related to the unknown dislocation density, $b(x, s)$, by the following integral equation

$$\int_{-\infty}^{0} \frac{b(x',s)}{s}\left(\frac{1}{(x-x')} + \frac{1}{\bar{\eta}}\left(-\frac{2\epsilon^2}{(x-x')^3} + \frac{2\epsilon K_1(|x-x'|/\epsilon)}{(x-x')|x-x'|} + \frac{K_0(|x-x'|/\epsilon)}{(x-x')}\right)\right) \mathrm{d}x' = \begin{cases} \bar{\sigma}_{12}(x,0,s) & \text{for } x \geqslant 0, \\ -\tau_0 \mathrm{e}^{x/a}/s & \text{for } x < 0. \end{cases} \tag{2.8}$$

The integral above must be interpreted in the Cauchy principal value sense, the expressions $K_0(z), K_1(z)$ denote modified Bessel's functions, and $\overline{\sigma}_{12}$ represents the unknown stress distribution ahead of the crack. We have defined $\epsilon$ as $\epsilon = (c/s)^{1/2}$. The integral equation is derived from the dislocation solutions of Appendix C, in particular the Laplace transformed shear stress on the glide plane for a dislocation with constant dislocation density, $b$, is

$$\overline{\sigma}_{12}(x,0,s) = \frac{b}{s}\left(\frac{1}{x} + \frac{1}{\overline{\eta}}\left(-\frac{2\epsilon^2}{x^3} + \frac{2\epsilon}{x|x|}K_1(|x|/\epsilon) + \frac{1}{x}K_0(|x|/\epsilon)\right)\right). \tag{2.9}$$

By using dislocation solutions in real time it would be possible to write the integral equation (2.8) in an even more explicit form involving an integral with respect to a time variable; for the method we use here there is no advantage in this. The terms in the kernel of integral equation (2.8) correspond to the usual Cauchy singular elastic kernel and terms involving modified Bessel's functions; these can be identified as being generated by dipoles orientated to satisfy the pore pressure boundary condition. Finally there is a dilatational response to these dipoles. Although this integral equation may appear to be hypersingular as $x \to x'$, the overly singular parts cancel, and the integral equation is Cauchy singular. In the dislocation solutions fluid and elastic responses can be separated and the terms in the kernel can be identified as due to elastic or fluid responses. We consider crack problems here and elsewhere; these crack problems will not uncouple in such a simple fashion. The aim is to identify, at least for small times, the sequence of responses which drive the stress intensity factor (2.6). To solve this integral equation we work in both Fourier and Laplace transform space and define $\epsilon = (c/s)^{1/2}$. For small times $\epsilon$ is a small parameter we shall use this extensively.

Initially, we subtract out the applied loading in the undrained elastic limit, we simply approximate the kernel by taking the limit for small $\epsilon$ and obtain the dislocation density for this simpler problem. However, by doing this we expect to make an error near the crack tip, so we subtract off this first solution from the full problem, scale on the small parameter, and solve this new problem. This 'inner' solution corrects for the approximation we previously made. We proceed by going back to unscaled variables, subtracting off the solution we have corrected for already, and solving the resulting problem to the required order. We scale on the small parameter and solve the 'inner' problem and repeat this back and forth process correcting each time for the approximations we have made. Corrected solutions for the field variables are given by the sum of these 'inner' solutions.

Fourier transforming (2.8), using the dislocation solutions from Appendix C in both Fourier and Laplace transform space, we use the half range transforms for the shear stress

$$\tau_+ = \int_0^\infty \overline{\sigma}_{12}(x,0,s)e^{i\chi x}\,dx, \tag{2.10}$$

and the transformed dislocation density

$$b_- = \int_{-\infty}^0 b(x,s)e^{i\chi x}\,dx, \tag{2.11}$$

to deduce the following functional equation

$$\tau_+ - \frac{\tau_0 a}{s(1+i\chi a)} = \frac{\pi b_- i|\chi|\epsilon^2}{s\chi\overline{\eta}}\left(\chi^2 - |\chi|(\chi^2+\epsilon^{-2})^{1/2} + \overline{\eta}/\epsilon^2\right). \tag{2.12}$$




PHILOSOPHICAL TRANSACTIONS OF THE ROYAL SOCIETY A MATHEMATICAL, PHYSICAL & ENGINEERING SCIENCES

The subscripts + and − denote functions that are analytic in the upper and lower complex $\chi$ planes (where $\chi$ is the Fourier transform parameter) respectively, we have not scaled the variables to remove the $s$ dependence from the kernel (this is the last bracketed term of (2.12)); this is the full problem written in unscaled variables. The main advantage with working with these equations derived from a distribution of dislocations is that they will automatically satisfy the pore pressure boundary conditions and are an alternative method of generating the Wiener–Hopf type equations considered previously by the authors. It is clear we could proceed as in §2 to get the full solution almost immediately, but let us instead proceed as described above.

Initially, we solve the functional equation (2.12) in the limit as $\epsilon \to 0$. For these outer problems we define $\tau_+^{(j)}$ to be the term in the expression for the transformed shear stress which contains terms of order $\epsilon^{j/2}$ and anticipate that the transformed shear stress can be written as an expansion in powers of $\epsilon$, i.e.

$$\tau_+ \sim \tau_+^{(0)} + \tau_+^{(2)} + \tau_+^{(4)} + \cdots . \tag{2.13}$$

A similar notation is used for the transformed dislocation density, $b_-^{(j)}$.

Unfortunately these outer problems do not solve the problem correctly at each order and a correction is required. For the inner problems we now scale on $\epsilon$ by defining a new Fourier transform variable as $\xi = \epsilon\chi$. The transformed integral equation (2.12) is rewritten in terms of this rescaled transform variable. The parts of the transformed integral equation which have been solved to the order to which we are working are subtracted off, and the remaining functional equation is solved. The notation we use for the expansions of the outer transformed shear stress, $\tau_+^{(j)}$, in the inner transform variable is $\Upsilon_+^{(j,i)}$. The superscript $i$ denotes the expansion (in the inner variable) is taken to order $\epsilon^{(i+1)/2}$. The unknown transformed shear stress which is the correction term of order $\epsilon^{(i+1)/2}$ is denoted by $\Upsilon_+^{(j+1,i)}$ at each step. If any logarithmic terms appear, i.e. $\epsilon^{(i+1)/2}(\log\epsilon)^n$, these are grouped together with the term involving $\epsilon^{(i+1)/2}$. A similar notation is used for the transformed dislocation density that, in the inner problem, is written $B_-^{(j,i)}$.

The outer fields give the transform solutions away from the crack tip and are used to interpret how the crack appears in the far field. When written in the inner transform variable and combined with the inner corrections they give the full solution to the problem to a particular order. For instance the transformed stress to order $\epsilon^{1/2}$ in the inner variables is given by

$$\Upsilon_+^{(0,0)} + \Upsilon_+^{(1,0)}.$$

The term $\Upsilon_+^{(0,0)}$ comes from the first term in the expansion of $\tau_+^{(0)}$ in the inner variable and $\Upsilon_+^{(1,0)}$ comes from a functional equation which corrects for the non-uniformity to this order.

We now apply the method. In the unscaled (outer) equation, (2.12), we take the limit as $s \to \infty$ and solve the following problem

$$\tau_+^{(0)} - \frac{\tau_0 a}{s(1+i\chi a)} = \frac{\pi b_-^{(0)} \mathrm{i}\chi}{|\chi| s}. \tag{2.14}$$

This is just the equivalent elastic problem (with undrained Poisson's ratio), and represents the problem in the far field in the limit of small times. This involves the Fourier transform of the usual Cauchy singular integral for elasticity, i.e.

$$\int_{-\infty}^{0} \frac{b^{(0)}(x',s)}{s(x-x')}\,\mathrm{d}x' = \begin{cases} \overline{\sigma}_{12}^{(0)}(x,0,s) & \text{for } x \geqslant 0, \\ -\tau_0 \mathrm{e}^{x/a}/s & \text{for } x < 0. \end{cases} \tag{2.15}$$

Physically the fluid would not have had time to diffuse, hence in the far field the problem appears to be a loaded crack in an elastic material (with undrained moduli). This can be solved using standard Wiener–Hopf techniques to give the following functional equation

$$\frac{\tau_+^{(0)}}{\chi_+^{1/2}} - \frac{\tau_0 a}{s(1+\mathrm{i}\chi a)}\left(\frac{1}{\chi_+^{1/2}} - \frac{1}{(\mathrm{i}/a)_+^{1/2}}\right) = \frac{\pi b_-^{(0)}\mathrm{i}}{s\chi_-^{1/2}} + \frac{\tau_0 a}{s(1+\mathrm{i}\chi a)(\mathrm{i}/a)_+^{1/2}} = 0. \tag{2.16}$$

This functional equation gives us solutions for $\tau_+^{(0)}, b_-^{(0)}$. These are written in the inner coordinates to give

$$\Upsilon_+^{(0,4)} = -\frac{\tau_0\epsilon^{1/2}}{s(\mathrm{i}/a)_+^{1/2}\mathrm{i}\xi_+^{1/2}} + \frac{\tau_0\epsilon}{s\mathrm{i}\xi} - \frac{\tau_0\epsilon^{3/2}}{s\xi_+^{3/2}a(\mathrm{i}/a)_+^{1/2}} + \frac{\tau_0\epsilon^2}{s\xi^2 a} + \frac{\tau_0\epsilon^{5/2}}{\mathrm{i}s(\mathrm{i}/a)_+^{1/2}\xi_+^{5/2}a^2}, \tag{2.17}$$

$$\pi B_-^{(0,4)} = \frac{\tau_0\epsilon^{1/2}}{(\mathrm{i}/a)_+^{1/2}\xi_-^{1/2}} - \frac{\tau_0\epsilon^{3/2}}{\mathrm{i}\xi_-^{3/2}a(\mathrm{i}/a)_+^{1/2}} - \frac{\tau_0\epsilon^{5/2}}{(\mathrm{i}/a)_+^{1/2}a^2\xi_-^{5/2}}. \tag{2.18}$$

Clearly this solution will be incorrect to leading order from the approximation we have made to the kernel, because of the non-uniform limit as $\epsilon \to 0$ and $x \to 0$, so we subtract (2.14) from the full problem and now solve

$$\Upsilon_+^{(1,0)} - \frac{\pi B_-^{(0,0)}\mathrm{i}|\xi|}{s\overline{\eta}\xi}(\xi^2 - (\xi^2+1)^{1/2}|\xi|) = \frac{\pi B_-^{(1,0)}\mathrm{i}|\xi|}{s\overline{\eta}\xi}N(\xi). \tag{2.19}$$

In (2.19) we now switch to 'inner' coordinates defined by $\chi\epsilon = \xi$; $\epsilon = (c/s)^{1/2}$ is our small parameter and recall that $N(\xi) = \xi^2 - |\xi|(\xi^2+1)^{1/2} + \overline{\eta}$. Note that equation (2.19) combined with (2.14) would still be the exact problem; if we replaced $B_-^{(0,0)}$ by $b_-^{(0)}$, no approximation would have been made. We solve (2.19) to get the following functional equation

$$\frac{\Upsilon_+^{(1,0)}}{\xi_+^{1/2}N_+} + \frac{\tau_0\mathrm{i}\epsilon^{1/2}}{\xi s(\mathrm{i}/a)_+^{1/2}}\left(\frac{1}{N_+} - \frac{1}{N_+(0)}\right)$$

$$= \frac{\pi B_-^{(1,0)}\mathrm{i}N_-}{s\overline{\eta}\xi_-^{1/2}} + \frac{\tau_0\mathrm{i}\epsilon^{1/2}}{\xi s(\mathrm{i}/a)_+^{1/2}}\left(\frac{N_-}{\overline{\eta}} - \frac{1}{N_+(0)}\right) = 0, \tag{2.20}$$

where the pole from $1/\xi$ is taken to lie in the minus region. This is because it comes from taking the limit in a minus function. The approximation we have taken is equivalent to the loading appearing uniform in the inner region. Now summing the contribution of the 'inner' limits for the stress we deduce that the transformed stress corrected to this order is given by

$$\Upsilon_+^{(0,0)} + \Upsilon_+^{(1,0)} = \mathrm{i}\tau_0\epsilon^{1/2}N_+/s\xi_+^{1/2}(\mathrm{i}/a)_+^{1/2}N_+(0). \tag{2.21}$$





PHILOSOPHICAL TRANSACTIONS OF THE ROYAL SOCIETY A MATHEMATICAL, PHYSICAL & ENGINEERING SCIENCES

Hence, the mode 2 stress intensity factor is given (to this order) by

$$\overline{K}_{\mathrm{II}}(s) = \tau_0 a^{1/2}\sqrt{2}/sN_+(0), \tag{2.22}$$

which is precisely the leading order term in (2.7) obtained previously. The method gives us corrections to the dislocation density and hence the corrections to all the variables of interest.

Now we continue the method to give the next terms. We go back to the outer variable $\chi$ and solve

$$\tau_+^{(2)} = \frac{\pi b_-^{(2)}\mathrm{i}|\chi|}{s\chi} - \frac{\mathrm{i}\epsilon\chi}{s\overline{\eta}}\pi(b_-^{(0)} - B_-^{(0,0)}). \tag{2.23}$$

The first term on the right-hand side is the next outer solution and the second term comes from the next term in the expansion of the kernel combined with $b_-^{(0)} - B_-^{(0,0)}$ as we have already corrected for $B_-^{(0,0)}$ in our previous inner solution. The term $B_-^{(0,0)}$ is written in terms of the outer variable $\chi$. This corresponds to an induced loading of the crack by a distribution of dipoles orientated to maintain the pore pressure boundary condition on the crack faces. In real space this is the following integral equation

$$\int_{-\infty}^{0} -\frac{2\epsilon\tau_0 D((-x'/a)^{1/2})}{\overline{\eta}s\sqrt{\pi}}\pi\delta'(x-x') + \frac{b^{(2)}(x',s)}{s(x-x')}\,\mathrm{d}x' = \begin{cases}\overline{\sigma}_{12}^{(2)}(x,0,s) & \text{for } x \geqslant 0,\\ 0 & \text{for } x < 0.\end{cases} \tag{2.24}$$

The function $\delta(x)$ denotes the Dirac delta function and can be regarded as representing a point source, the generalized function $\delta'(x)$ corresponds to a point dipole. The following result from generalized function theory has been used, in the limit as $a \to \infty$

$$\frac{1}{\pi}\left(\frac{2}{x|x|}K_1(a|x|) + a\frac{K_0(a|x|)}{x}\right) = \delta'(x). \tag{2.25}$$

The integral involving $\delta'(x)$ can be found explicitly, but there seems no advantage for the method we use here in doing so. It is perhaps easier to understand the approximation using this integral equation. The first term is the corrected dislocation density for the elastic loading (where $D(x)$ is Dawson's integral, see Appendix A) acting to induce a distribution of dipoles. The second term is just the Cauchy singular integral equation for elasticity, which will give the next term in the dislocation density to correct for the new loading. Returning to (2.23), we require the sum split of a term $|\chi|((1+\mathrm{i}\chi a)^{-1} - (\mathrm{i}\chi a)^{-1})$ which we denote by $C(\chi)$. By contour integration $C_\pm(\chi)$ is given by

$$C_\pm(\chi) = \mp\frac{1}{\pi a}\frac{\log(\mp\mathrm{i}\chi a)}{(1+\mathrm{i}\chi a)}. \tag{2.26}$$

This sum split suggests the diffusion of pore fluid is altering the loading on the crack and the sum split is rearranging this loading. The functional equation is deduced in a similar manner to those previously. The correction to the dislocation density $b_-^{(2)}$ and stress $\tau_+^{(2)}$ is given by

$$\pi b_-^{(2)} = -\frac{\epsilon\tau_0 a C_-(\chi)\chi_-^{1/2}}{\overline{\eta}\mathrm{i}(\mathrm{i}/a)_+^{1/2}}, \quad \tau_+^{(2)} = \frac{\epsilon\tau_0 a\chi_+^{1/2}C_+(\chi)}{s\overline{\eta}(\mathrm{i}/a)_+^{1/2}}. \tag{2.27}$$

These transforms can be inverted using (A 5) of Appendix A if required. We deduce $\Upsilon_+^{(2,j)}, B_-^{(2,j)}$ from (2.27) by rewriting (2.27) in the inner variable and taking the limit as $\epsilon$ tends to zero. Returning to inner variables we wish to correct for any error which has been made in this approximation; we deduce the following functional equation for the next order correction

$$\Upsilon_+^{(3,2)} = \frac{\mathrm{i}|\xi|}{s\xi\overline{\eta}}(N - \overline{\eta} + |\xi|)\pi(B_-^{(0,2)} - B_-^{(0,0)}) + \frac{\mathrm{i}|\xi|}{s\overline{\eta}\xi}(N - \overline{\eta})\pi B_-^{(2,2)} + \frac{\mathrm{i}|\xi|}{s\xi\overline{\eta}}N\pi B_-^{(3,2)}. \tag{2.28}$$

After suitable rearrangement, so the Wiener–Hopf technique can be applied, we find the stress $\Upsilon_+^{(3,2)}$ is given by

$$\Upsilon_+^{(3,2)} = \frac{\tau_0\epsilon^{3/2}}{sa(\mathrm{i}/a)_+^{1/2}}\Big(\xi_+^{-3/2}(1 - N_+/N_+(0)) + \frac{\mathrm{i}N_+}{N_+(0)\xi_+^{1/2}}(n_{11} + n_{12}\log(\epsilon/2a)) - (\mathrm{i}/\xi_+^{1/2})n_{12}\log(\epsilon/2a)\Big). \tag{2.29}$$

To deduce the above we have subtracted out both the simple and double poles, which come from a minus function, and we have used the sum split for

$$\frac{1}{|\xi|} = \frac{1}{\pi\mathrm{i}\xi}(\log(\mathrm{i}\xi) - \log(-\mathrm{i}\xi)).$$

We now consider the full expression for the corrected stress to order $\epsilon^{3/2}$ in the inner transform variable as $\Upsilon_+^{(0,2)} + \Upsilon_+^{(1,0)} + \Upsilon_+^{(2,2)} + \Upsilon_+^{(3,2)} = \Upsilon_+^{3/2}$, where

$$\Upsilon_+^{3/2} = \frac{\tau_0 N_+}{s(\mathrm{i}/a)_+^{1/2}N_+(0)} \times \left(\frac{\mathrm{i}\epsilon^{1/2}}{\xi_+^{1/2}} + \frac{\epsilon^{3/2}}{a}\left(-\frac{1}{\xi_+^{3/2}} + \frac{\mathrm{i}}{\xi_+^{1/2}}(n_{11} + n_{12}\log(\epsilon/2a))\right)\right) + \frac{\tau_0\epsilon}{s\mathrm{i}\xi}. \tag{2.30}$$

By using corrections for the dislocation densities we can find the corrections for any other field variables. We now proceed in a similar fashion to deduce the next order term by returning to outer variables and solving the following functional equation

$$\tau_+^{(4)} = \pi(b_-^{(0)} - B_-^{(0,2)})\frac{\mathrm{i}|\chi|\epsilon^2\chi}{s\overline{\eta}} - \pi(b_-^{(2)} - B_-^{(2,2)})\frac{\mathrm{i}\epsilon\chi}{s\overline{\eta}} + \pi b_-^{(4)}\frac{\mathrm{i}|\chi|}{s\chi}. \tag{2.31}$$

This equation is now the full equation with the approximations and the parts of the kernel for which they are the solutions subtracted off. In real space it is the following integral equation for $b^{(4)}$,

$$\int_{-\infty}^{0} \frac{4\epsilon^2\tau_0}{\overline{\eta}(x-x')^3\sqrt{\pi}}(D((-x'/a)^{1/2})-(-x'/a)^{1/2}) - \frac{2\epsilon^2\tau_0 D_l((-x'/a)^{1/2})}{\pi\overline{\eta}a\sqrt{\pi}}\pi\delta'(x-x') + \frac{b^{(4)}(x',s)}{s(x-x')}\,\mathrm{d}x' = \begin{cases}\overline{\sigma}_{12}^{(4)}(x,0,s) & \text{for } x \geqslant 0,\\ 0 & \text{for } x < 0.\end{cases} \quad (2.32)$$

The function $D_l(x)$ is defined in Appendix A. The first term is interpreted as the dilatational response to the dipoles induced by the elastic loading. The second term is interpreted as a corrected distribution of dipoles, these are induced by the loading which comes from the correction to the original elastic loading. The final term is the usual Cauchy singular elastic integral equation, this contains the dislocation density which will correct for the sum of these different loadings. We return to (2.31) and solve this equation after the factorization for the sum split of $E(\chi)$ has been performed; $E(\chi)=\log(\mathrm{i}\chi a)C(\chi)$, i.e.

$$E(\chi) = \frac{1}{2\pi a(1+\mathrm{i}\chi a)}(\log^2(\mathrm{i}\chi a) - \pi^2 - \log^2(-\mathrm{i}\chi a)). \quad (2.33)$$

The split function $E_+(\chi) = -\log^2(-\mathrm{i}\chi a)/2\pi a(1+\mathrm{i}\chi a)$ and the minus function is given by $E_-(\chi) = E(\chi) - E_+(\chi)$. Solving (2.31) we find

$$\tau_+^{(4)} = -\frac{\tau_0\epsilon^2\chi_+^{1/2}\log^2(-\mathrm{i}\chi a)}{2s\pi^2\overline{\eta}^2(\mathrm{i}/a)_+^{1/2}a(1+\mathrm{i}\chi a)}, \quad (2.34)$$

this can be inverted using results from Appendix A. A similar expression for $\pi b_-^{(4)}$ can also be deduced; by rewriting these in the inner variables and expanding, we find their inner approximations $\Upsilon_+^{(4,4)}, \pi B_-^{(4,4)}$. These approximations will be incorrect in the neighbourhood of the crack tip, so we return to the inner variables and solve

$$\Upsilon_+^{(5,4)} = (\mathrm{i}|\xi|\pi/s\xi\overline{\eta})((b_-^{(0)} - B_-^{(0,2)})(N-\overline{\eta}+|\xi|-\xi^2) + (b_-^{(2)} - B_-^{(2,2)})(N-\overline{\eta}+|\xi|) + B_-^{(4,4)}(N-\overline{\eta}) + B_-^{(5,4)}N). \quad (2.35)$$

The above functional equation is rearranged in the usual Wiener–Hopf manner to give the corrections to the stresses and dislocation densities. We obtain a full expression for the corrected stresses to order $\epsilon^{5/2}$ as

$$\Upsilon_+^{(0,4)} + \Upsilon_+^{(1,0)} + \Upsilon_+^{(2,4)} + \Upsilon_+^{(3,2)} + \Upsilon_+^{(4,4)} + \Upsilon_+^{(5,4)},$$

this is

$$\Upsilon_+^{5/2} = \Upsilon_+^{3/2} + \frac{\tau_0\epsilon^2}{sa\xi^2} + \frac{\tau_0\epsilon^{5/2}\mathrm{i}N_+}{sa^2(\mathrm{i}/a)_+^{1/2}N_+(0)}\Big(-\xi_+^{-5/2} + \frac{\mathrm{i}}{\xi_+^{3/2}}(n_{11}+n_{12}\log(\epsilon/2a)) - \xi_+^{-1/2}((n_{21}-n_{11}^2) + (n_{11}/\pi\overline{\eta})\log(\epsilon/2a) - n_{23}\log^2(\epsilon/2a))\Big). \quad (2.36)$$

The limit of (2.36) as $|\xi| \to \infty$, suitably rescaled, is used to give an asymptotic expression for the Laplace transformed stress intensity factor. This is inverted using the Laplace transforms given in Appendix A to give the asymptotic expansion for the stress intensity factor in real time, i.e. (2.7).

We now interpret the result in the following manner. The outer field is initially that of an undrained elastic material with the same applied loading. To the next order this is corrected for (to maintain the permeable boundary condition on the crack faces) by a distribution of dipoles related to this initial loading. These dipoles in turn redistribute the load on the crack, allowing a further approximation to be performed. The final-order outer solution is a combination of the loading induced by the earlier dipoles inducing a correction to this dipole distribution, together with a dilatation term which balances the pore pressure induced on the fracture plane by the elastic loading. This outer solution has been found using a rigorous asymptotic analysis of the integral equations. So we have been able to partly uncouple the elastic and pore pressure responses for this problem. We must emphasize the method outlined above is not designed to evaluate the stress intensity factor for this particular problem in the most efficient manner (this is done in [CA]), but to isolate the physical processes that are driving the field variables and to obtain a real time asymptotic solution for the stress intensity factor. We also want to verify that the method we intend to use for approximating the kernel of the integral equation in inner and outer limits does indeed check against existing results. The real time evaluation of the stress intensity factor is valuable as we obtain an explicit formula requiring no numerical inversion of Laplace transforms. In a later section this is illustrated by considering a crack with a point load applied to the crack faces at specified distance from the crack tip.

Similar results can be deduced for the other unmixed case, a semi-infinite crack with impermeable crack faces loaded under tension, equation (85) of [CA]; the asymptotic results for the impermeable kernel function $\overline{N}(\xi)$ are required from Appendix A. In this case the asymptotic expansion for the mode 1 stress intensity factor for the impulsively introduced exponentially decaying loading is given by

$$K_1(t') = \frac{\sqrt{2}a^{1/2}\tau_0}{\overline{N}_+(0)}(H(t') + 2(t'/\pi)^{1/2}\overline{n}_1 + t'(\overline{n}_2 + \overline{n}_1^2) + \frac{4t'^{3/2}}{3\pi^{1/2}}(\overline{n}_1^3 + \mathrm{i}\overline{n}_3 + 2\overline{n}_1\overline{n}_2) + \frac{2t'^{3/2}}{3\pi^{1/2}\pi\overline{\eta}}(\log(t') + \gamma - \tfrac{8}{3}) + \cdots). \tag{2.37}$$

The appropriate constants are given in Appendix A. Note that to order $t'$ there is no logarithmic contribution; this comes in at order $t'^{3/2}$. A similar analysis to that for the other unmixed case can be performed. The order of events is as follows: initially the outer field is that of an undrained elastic material, this gives us the same first order term as in the case considered above. To the next order a distribution of dipoles, related to the elastic loading, orientated along the crack to maintain the pore pressure boundary condition on the crack are induced. These, in turn, induce a dilatation and it is this which gives the next term in the outer field. The explicit dipole response (i.e. the logarithmic terms) comes in at a higher order.

### (b) *An asymptotic approach for small s*

Looking at the integral equation (2.12) it is also clear we could attempt to perform an asymptotic small $s$ analysis. To proceed we define $\delta = 1/\epsilon$, $\delta$ is now the appropriate small parameter. By Fourier transforming (2.8) and using the dislocation solutions, from Appendix C, in both Fourier and Laplace transform space we deduce the following relation between the half range transforms for the shear stress, $\tau_+$ and the transformed dislocation density, $b_-$

$$\tau_+ - \frac{\tau_0 a}{s(1+\mathrm{i}\chi a)} = \frac{\pi b_- \mathrm{i}|\chi|}{s\chi\overline{\eta}\delta^2}(\chi^2 - |\chi|(\chi^2+\delta^2)^{1/2} + \overline{\eta}\delta^2). \tag{2.38}$$

This is solved in the limit as $\delta \to 0$ to yield the following functional equation for the stress and dislocation density

$$\tau_+^{(0)} - \frac{\tau_0 a}{s(1+\mathrm{i}\chi a)} = \frac{\pi b_-^{(0)} \mathrm{i}|\chi|}{s\chi}\frac{(1-\nu_\mathrm{u})}{(1-\nu)}. \tag{2.39}$$

The ratio of $1-\nu_\mathrm{u}$ to $1-\nu$ arises as the dislocation solutions are derived using the undrained moduli. In real space this is the usual Cauchy singular equation for elasticity, i.e.

$$\int_{-\infty}^{0} \frac{(1-\nu_\mathrm{u})}{(1-\nu)}\frac{b^{(0)}(x',s)}{s(x-x')}\,\mathrm{d}x' = \begin{cases} \overline{\sigma}_{12}^{(0)}(x,0,s) & \text{for } x \geqslant 0, \\ -\tau_0 \mathrm{e}^{x/a}/s & \text{for } x < 0. \end{cases} \tag{2.40}$$

This is simply the elastic problem with drained Poisson's ratio. This corresponds to the physical situation a long time after loading when the excess pore pressure created by the loading will have equilibrated. However, the equations are non-uniform in the limit as $\delta \to 0$ and $x \to \infty$, this is the reverse of the non-uniformity which arose in the small times analysis. To correct for this we subtract out the elastic solution from the full problem and then rescale. The rescaling chosen is that the outer coordinate $X = \delta x$, this rescales our Fourier transform variable, so we define $\xi = \chi/\delta$. Physically this rescaling corresponds to reducing the crack problem and magnifying the problem at infinity. For small times this rescaling magnifies the crack problem and it is the 'inner' problem. For the large time approach this outer problem is

$$\Upsilon_+^{(1,0)} = -\frac{\tau_0 a \xi_+^{1/2}\delta^{1/2}}{s(\mathrm{i}/a)_+^{1/2}\overline{\eta}}(N - (\overline{\eta} - \tfrac{1}{2})) + \frac{\pi B_-^{(1,0)}\mathrm{i}|\xi| N}{s\xi\overline{\eta}}. \tag{2.41}$$

We have used in this equation the leading order, in $\delta$, behaviour of the elastic dislocation density. We note that if we take the full elastic dislocation density in the first term of (2.41) instead of $B_-^{(0,0)}$ then the addition of (2.39) and (2.41) is the full problem and no approximation would have made. The problem solved here will be accurate to $O(\delta)$, solving (2.41) using standard Wiener–Hopf methods, gives

$$\frac{\Upsilon_+^{(1,0)}}{\xi_+^{1/2}N_+} - \frac{\tau_0 a\delta^{1/2}}{s(\mathrm{i}/a)_+^{1/2}N_+} = -\frac{\tau_0 a \delta^{1/2} N_-}{s(\mathrm{i}/a)_+^{1/2}(\overline{\eta}-\frac{1}{2})} + \frac{\pi B_-^{(1,0)} iN_-}{s\xi_-^{1/2}\overline{\eta}} = -\frac{\tau_0 a\delta^{1/2}}{s(\mathrm{i}/a)_+^{1/2}}. \tag{2.42}$$

We use this, and the asymptotic behaviour of the transform, $N_+$, as $\xi \to \infty$, i.e

$$N_+(\xi) \sim 1 - \frac{\mathrm{i}}{\pi\xi}\int_0^1 \arctan\left(\frac{p(1-p^2)^{1/2}}{p^2-\overline{\eta}}\right)\mathrm{d}p, \tag{2.43}$$

to identify the correction term. Utilising an Abelian result for the transforms (the limit as $\xi \to \infty$, is analogous to $X \to 0$ in real space) we identify the near crack tip results which in turn gives the corrected large time stress intensity factor in real time as

$$K_{\mathrm{II}}(t') \sim \sqrt{2}a^{1/2}\tau_0 \left(H(t') + (\pi^{3/2}t'^{1/2})^{-1}I + O(1/t') + \cdots\right) \tag{2.44}$$

and $I$ is given by

$$I = \int_0^1 \arctan\left(\frac{p(1-p^2)^{1/2}}{p^2-\overline{\eta}}\right) \mathrm{d}p = 1 - \frac{\overline{\eta}}{(2\overline{\eta}-1)^{1/2}} \arctan\left(\frac{(2\overline{\eta}-1)^{1/2}}{\overline{\eta}-1}\right). \tag{2.45}$$

The non-dimensional timescale $t' = tc/a^2$. The stress intensity factor is plotted versus the full numerical solution from Craster & Atkinson (1992*b*) and the small time asymptotic solution from above in figure 1 (for $\nu = 0.3$, $\nu_{\mathrm{u}} = 0.4$). The solution is now adequately described by the asymptotics, picking up both the increase in, and the levelling off of, the stress intensity factor.

## 3. A mixed problem

In previous papers [CA] and [AC] the emphasis has been on more complicated problems that have mixed boundary conditions for the pore pressure on the fracture plane. One example of this is a permeable crack opening under a tensile loading, with the fracture plane ahead of the crack having an impermeable boundary condition due to the symmetry of the problem. Such a situation can occur in the hydraulic fracture process, where one is propagating a fracture into virgin rock. Such mixed problems are also required for a full study of cracks in arbitrary stress fields. Consider a permeable crack subjected to an arbitrary stress field. The stress field can be decomposed into a shear and a tensile component. When considered individually, one has a shear loaded permeable crack (an unmixed problem, see § 2) and the tensile loaded permeable fracture (a mixed problem). The aim of this section is to modify the asymptotic procedure so it can be applied to these mixed problems and to try to understand what is happening at the crack tip.

As in § 2, we formulate the problem by considering the crack as being made of a distribution of dislocations. In this case we use a distribution of impermeable dislocations as these will have the appropriate pore pressure condition ahead of the crack tip. We use a distribution of pore pressure gradient discontinuities to annul the induced pore pressure along the crack faces, thereby maintaining the permeable crack faces condition. We have two coupled integral equations to solve, giving the pore pressure and tensile stress in terms of these distributions. These integral equations are combined into a single integral equation which is solved separately. The stress intensity factor is determined via the integral equation for the pore pressure using the constraint that the pore pressure is not singular at the crack tip. This constraint comes from physical considerations; a singular pore pressure would lead to an infinite value for the energy at the crack tip, hence we require the pore pressure to be non-singular. To formulate the integral equations we require the opening dislocation and pore pressure gradient discontinuity solutions from Appendix C.

The specific problem we will treat here is the problem considered in [AC]. Let us consider a permeable crack with an internally applied tensile loading, so the boundary conditions are, on $y=0$,

$$p(x,y,t)=0,\quad \sigma_{22}(x,y,t)=-\tau_0 \mathrm{e}^{x/a}H(t) \text{ for } x<0, \tag{3.1}$$

$$\sigma_{12}(x,y,t)=0\ \forall\ x, \tag{3.2}$$

$$\partial p(x,y,t)/\partial y=0,\quad u_2(x,y,t)=0 \text{ for } x>0. \tag{3.3}$$

In the Laplace transformed domain the integral equations are

$$\frac{3\overline{p}(x,0,s)}{2B(1+\nu_{\mathrm{u}})}H(x)=\frac{1}{s}\int_{-\infty}^{0}-q(x',s)K_0\left(\frac{|x-x'|}{\epsilon}\right)$$
$$+\,b(x',s)\left(\frac{\operatorname{sgn}(x-x')}{\epsilon}K_1\left(\frac{|x-x'|}{\epsilon}\right)-\frac{1}{(x-x')}\right)\mathrm{d}x', \tag{3.4}$$

$$\frac{1}{s}\int_{-\infty}^{0}\frac{q(x',s)}{\overline{\eta}}\left(-\frac{\epsilon^2}{(x-x')^2}+\frac{\epsilon}{|x-x'|}K_1(|x-x'|/\epsilon)+K_0(|x-x'|/\epsilon)\right)$$
$$+\frac{b(x',s)}{(x-x')}+\frac{b(x',s)}{\overline{\eta}}\left(\frac{2\epsilon^2}{(x-x')^3}-\frac{2\epsilon K_1(|x-x'|/\epsilon)}{(x-x')|x-x'|}\right.$$
$$\left.-\frac{K_0(|x-x'|/\epsilon)}{(x-x')}-\operatorname{sgn}(x-x')\frac{K_1(|x-x'|/\epsilon)}{\epsilon}\right)\mathrm{d}x'$$
$$=\begin{cases}\overline{\sigma}_{22}(x,0,s), & x\geqslant 0,\\ -\tau_0\mathrm{e}^{x/a}/s, & x<0.\end{cases} \tag{3.5}$$

In the above $q(x',s)$ and $b(x',s)$ are unknown distributions of pore pressure gradient discontinuities and dislocation densities respectively, and $\overline{p}(x,0,s)$, $\overline{\sigma}_{22}(x,0,s)$ are the unknown pore pressure and stress ahead of the crack. We note here as an aside that if we were to set $q(x',s)$ to be zero in (3.5) above, this would be the integral equation for the tensile problem where the crack is assumed to have impermeable crack faces, i.e. the tensile, unmixed analogue of § 2.

Returning to the present problem and using half range Fourier transforms, i.e.

$$P_+=\int_0^\infty \overline{p}(x,0,s)\mathrm{e}^{\mathrm{i}\chi x}\,\mathrm{d}x,\quad T_+=\int_0^\infty \overline{\sigma}_{22}(x,0,s)\mathrm{e}^{\mathrm{i}\chi x}\,\mathrm{d}x \tag{3.6}$$

(and minus transforms for the pore pressure gradient discontinuities and dislocation density defined as in (2.11)), the transformed integral equations are written

$$\frac{3P_+}{2B(1+\nu_{\mathrm{u}})}=-\frac{\pi q_-}{s(\chi^2+\epsilon^{-2})^{1/2}}+\frac{b_-\pi}{\mathrm{i}s}\left(\frac{|\chi|}{\chi}-\frac{\chi}{(\chi^2+\epsilon^{-2})^{1/2}}\right), \tag{3.7}$$

$$T_+-\frac{\tau_0 a}{s(1+\mathrm{i}\chi a)}=\frac{\pi b_-}{\mathrm{i}s}\left(\frac{\chi\epsilon^2}{\overline{\eta}}\left(|\chi|-\frac{\chi^2}{(\chi^2+\epsilon^{-2})^{1/2}}\right)-\frac{|\chi|}{\chi}\right)$$
$$+\frac{\pi q_-}{s}\frac{\epsilon^2}{\overline{\eta}}\left(|\chi|-\frac{\chi^2}{(\chi^2+\epsilon^{-2})^{1/2}}\right). \tag{3.8}$$

Combining (3.4) and (3.5) in the combination $\overline{\sigma}_{22}(x,0,s)+3\overline{p}(x,0,s)/2B(1+\nu_{\mathrm{u}})=$

$\overline{m}(x,0,s)$ gives the simpler integro-differential equation

$$-\frac{1}{s}\int_{-\infty}^{0}\left(q(x',s)+b(x',s)\frac{\partial}{\partial x}\right)\left(K_0(|x-x'|/\epsilon)(1-\overline{\eta}^{-1})\right.$$

$$\left.-\overline{\eta}^{-1}\left(\frac{\epsilon K_1(|x-x'|/\epsilon)}{|x-x'|}-\frac{\epsilon^2}{(x-x')^2}\right)\right)\mathrm{d}x' = \begin{cases}\overline{m}(x,0,s) & \text{for } x \geqslant 0,\\ -\tau_0 \mathrm{e}^{x/a}/s & \text{for } x < 0,\end{cases} \tag{3.9}$$

and in the transform domain

$$M_+ - \frac{\tau_0 a}{s(1+\mathrm{i}\chi a)}$$

$$= -\frac{1}{(\chi^2+\epsilon^{-2})^{1/2}}\left(\frac{\chi\pi b_-}{\mathrm{i}s}+\frac{\pi q_-}{s}\right)\left(1+(\epsilon^2/\overline{\eta})(\chi^2-|\chi|(\chi^2+\epsilon^{-2})^{1/2})\right). \tag{3.10}$$

The half range transform $M_+$ is defined in a similar manner to (3.6). Equation (3.10) has many terms in common with (2.12) above. We note $\overline{\zeta}$ the transformed variation of fluid content is given by

$$\overline{\zeta}(\xi,y,s) = -\frac{1}{2G_{\mathrm{u}}\overline{\eta}s}\left(\pi q_- + \frac{\pi b_- \chi}{\mathrm{i}}\right)\frac{\mathrm{e}^{-(\chi^2+\epsilon^{-2})^{1/2}y}}{(\chi^2+\epsilon^{-2})^{1/2}}. \tag{3.11}$$

We could consider the function $\pi f_- = \pi q_- - \mathrm{i}\pi b_- \chi$ as being a distribution of point fluid sources along the crack. This can be used as the basis of a numerical method (see, for example, Detournay & Cheng 1987). It is easier to consider the problem using $\pi f_-$ and $\pi b_-$ as distributions of point sources and dislocations densities, although we should note $\pi f_-$ contains a term involving $\pi b_-$ so the distributions are coupled.

The equation (3.10) gives a direct relation between a 'plus' and 'minus' function. In [AC] and here, this relation is exploited to solve the full mixed problem. In [AC] the full problem is solved directly from the governing equations, a system of functional equations was derived which were solved using a subsidiary equation similar to (3.10). With systems of interrelated functional equations it is unusual to be able to solve the system using a reduction of this type, except in special cases where symmetries allow a reduction to a simpler problem; the physical reasons for the reduction in this case are now clearer. This subsidiary equation relates the combination of the applied loadings, $M_+$, to an unknown distribution of fluid sources which is multiplied by the permeable kernel (the unscaled $N(\xi)$ in [AC]). Thus, it represents the fluid variation caused by the interaction between the applied loading and the permeable crack face condition, the function $L_-$ defined in [AC] is now be seen to be equivalent to a distribution of point sources along the crack.

For the outer problems let us define $T_+^{(j)}, P_+^{(j)}$ and $M_+^{(j)}$ in the same way as we earlier defined $\tau_+^{(j)}$ in the discussion preceding (2.13). The same notation is used for the outer transformed dislocation density and pore pressure gradient discontinuity $b_-^{(j)}, f_-^{(j)}$. For the inner solutions we define $\Omega_+^{(i,j)}, \Pi_+^{(i,j)}, \mathcal{M}_+^{(i,j)}$ and $B_-^{(i,j)}, F_-^{(i,j)}$ as the inner transformed stress, pore pressure, split function, dislocation density and pore pressure gradient discontinuity fields respectively. We clearly have a more complicated system to solve, but the method is similar to that used earlier. We approximate the integral equations by taking the limit as $\epsilon \to 0$ in the outer variables, and solve the resulting equations. Then we scale on the inner variables and solve these equations to correct for any error made in the previous approximation. In the inner variables we work with the equation for $\overline{m}(x,0,s)$ (3.10) to identify the distribution of sources required and then substitute into the transformed pore pressure integral equation (3.7) to find the required distribution of dislocations. The constraint that the pore pressure is non-singular at the crack tip is used to determine the correction to the stress intensity factor via the edge conditions and the definition of $\overline{m}(x,0,s)$.

Initially, in the outer variables, we take the limit as $\epsilon \to 0$. Then the integral equation for the stress reduces to the usual Cauchy singular integral equation (2.15) with $\overline{\sigma}_{22}$ replacing $\overline{\sigma}_{12}$. The results (2.17) and (2.18) therefore still apply, with $\Omega_+^{(0,4)}$ replacing $\Upsilon_+^{(0,4)}$. The outer stress field is initially unaffected by the mixed pore pressure boundary conditions and the crack initially appears to lie in an undrained elastic material. We find the distribution of sources induced using the integral equation (3.9) for $\overline{m}(x,0,s)$ which in this outer limit is

$$-\frac{1}{s}\int_{-\infty}^{0} f^{(0)}(x',s)K_0(|x-x'|/\epsilon)\,\mathrm{d}x' = \begin{cases}\overline{m}^{(0)}(x,0,s) & \text{for } x \geqslant 0,\\ -\tau_0 \mathrm{e}^{x/a}/s & \text{for } x < 0.\end{cases} \tag{3.12}$$

Recall that $f(x',s)$ is the distribution of pore fluid sources, after Fourier transforming this integral equation we solve

$$M_+^{(0)} - \frac{\tau_0 a}{s(1+\mathrm{i}\chi a)} = -\frac{\pi f_-^{(0)}}{s(\chi^2+\epsilon^{-2})^{1/2}}. \tag{3.13}$$

Note in this problem we keep $(\chi^2+\epsilon^{-2})^{1/2}$ as a single term. The solution proceeds in a standard manner giving $f_-^{(0)}$ as

$$\frac{\pi f_-^{(0)}}{s} = \left(-\Sigma^{(0)} + \frac{\tau_0 a \mathrm{i}_+^{1/2}(\epsilon^{-1}+a^{-1})^{1/2}}{s(1+\mathrm{i}\chi a)}\right)(\chi - \mathrm{i}/\epsilon)^{1/2}. \tag{3.14}$$

The constant $\Sigma^{(0)}$ is determined from the edge conditions on the stress and pore pressure, from which it is determined in general that in the limit as $|\chi| \to \infty$ then $M_+ \sim T_+$ and $T_+ \sim \Sigma\chi_+^{-1/2}$. Therefore $\Sigma$ plays an important role as it is not only the constant which appears in the subsidiary equation, but also represents (in transform space) the leading order behaviour of the stress field. Hence $\Sigma^{(0)}$ is determined from $T_+^{(0)}$. Scaling on the inner variables determines $F_-^{(0,4)}$ as

$$\pi F_-^{(0,4)} = \frac{\tau_0 \Gamma_- \epsilon^{1/2}}{si(\mathrm{i}/a)_+^{1/2}} + \frac{\tau_0 \Gamma_- \mathrm{i}_+^{1/2}\epsilon^{3/2}}{si\xi}(\epsilon^{-1}+a^{-1})^{1/2} + \frac{\tau_0 \Gamma_- \mathrm{i}_+^{1/2}\epsilon^{5/2}}{s\xi^2 a}(\epsilon^{-1}+a^{-1})^{1/2}. \tag{3.15}$$

It is convenient to keep the terms $(\epsilon^{-1}+a^{-1})^{1/2}$ intact rather than expanding them explicitly for small $\epsilon$. We now move to the inner variables defined by $\xi = \epsilon\chi$ and subtract off the parts of the integral equations which have been solved to leave

$$\mathcal{M}_+^{(1,0)} = -\frac{\epsilon\pi F_-^{(1,0)}}{s}\frac{N}{\overline{\eta}\Gamma} - \frac{\epsilon\pi F_-^{(0,0)}}{s\Gamma}\left(\frac{N}{\overline{\eta}} - 1\right). \tag{3.16}$$

This is solved to give

$$\frac{\Gamma_+\mathcal{M}_+^{(1,0)}}{N_+} - \frac{\tau_0\epsilon^{1/2}}{\mathrm{i}s(\mathrm{i}/a)_+^{1/2}N_+} = -\frac{\epsilon N_-\pi F_-^{(1,0)}}{\overline{\eta}\Gamma_-} - \frac{\epsilon^{1/2}\tau_0 N_-}{\mathrm{i}s(\mathrm{i}/a)_+^{1/2}\overline{\eta}} = \Sigma^{(1,0)} - \frac{\tau_0\epsilon^{1/2}}{\mathrm{i}s(\mathrm{i}/a)_+^{1/2}}. \tag{3.17}$$

The constant $\Sigma^{(1,0)}$ will give us the correction to the stress intensity factor. Using the result for $\pi F_-^{(1,0)}$ we substitute this into the pore pressure integral equation. The resulting functional equation can be deduced

$$\frac{3\Pi_+^{(1,0)}}{2B(1+\nu_\mathrm{u})\xi_+^{1/2}} - \frac{\epsilon^{1/2}\tau_0}{\mathrm{i}s(\mathrm{i}/a)_+^{1/2}\Gamma_+\xi_+^{1/2}} - \overline{\eta}k_+\left(\Sigma^{(1,0)} - \frac{\tau_0\epsilon^{1/2}}{\mathrm{i}s(\mathrm{i}/a)_+^{1/2}}\right)$$

$$= \frac{\pi B_-^{(1,0)}}{\mathrm{i}s\xi_-^{1/2}} + \overline{\eta}k_-(\Sigma^{(1,0)} - \frac{\tau_0\epsilon^{1/2}}{\mathrm{i}s(\mathrm{i}/a)_+^{1/2}}) = -\overline{\eta}c_0(\Sigma^{(1,0)} - \frac{\tau_0\epsilon^{1/2}}{\mathrm{i}s(\mathrm{i}/a)_+^{1/2}}). \tag{3.18}$$

The function $k(\xi) = 1/N_-\Gamma_+\xi_+^{1/2}$ and is split into a sum of 'plus' and 'minus' functions in Appendix A. From the condition that the pore pressure is non-singular at the crack tip and using the asymptotic behaviour of $k_+$, $\Sigma^{(1,0)}$ can be deduced and hence the leading order stress intensity factor is determined as

$$K_1(t') \sim \frac{\tau_0 a^{1/2}\sqrt{2}}{\overline{\eta}(N_+(0)/\overline{\eta} - d)}H(t). \tag{3.19}$$

Returning to the outer variables we subtract out the first-order solutions and solve

$$T_+^{(2)} = \frac{\pi b_-^{(2)}}{\mathrm{i}s}\frac{|\chi|}{\chi}, \quad (\chi^2+\epsilon^{-2})^{1/2}M_+^{(2)} = -\frac{\pi f_-^{(2)}}{s} + \frac{\epsilon}{\overline{\eta}}|\chi|\frac{\pi}{s}(f_-^{(0)} - F_-^{(0,0)}). \tag{3.20}$$

The solution of these equations gives us the transformed dislocation density $b_-^{(2)}$ as $\pi b_-^{(2)} = 0$; the next order outer contribution to the stress intensity factor is zero. The source distribution is deduced to be

$$\pi f_-^{(2)} = \frac{\epsilon\chi}{\overline{\eta}\pi\mathrm{i}}\frac{\tau_0\mathrm{i}_+^{1/2}(a^{-1}+\epsilon^{-1})^{1/2}}{s(1+\mathrm{i}\chi a)}\log(\mathrm{i}\chi a)(\chi - \mathrm{i}/\epsilon)^{1/2}. \tag{3.21}$$

That the next term in the outer stress field is zero may appear rather surprising. Physically, the dipoles that are initially induced are orientated along the crack to maintain the pore pressure boundary condition ahead of the crack, and to this order do not affect the stress field. There is also a distribution of sources induced to negate the non-zero pore pressure on the crack faces. Returning to inner variables, we once more solve the integral equation for $\overline{m}(x,0,s)$,

$$-\frac{\Gamma}{\epsilon}\mathcal{M}_+^{(3,2)} = \frac{N\pi F_-^{(3,2)}}{\overline{\eta}} + \left(\frac{N}{\overline{\eta}} - 1\right)\pi F_-^{(2,2)} + \left(\frac{N}{\overline{\eta}} - 1 + \frac{|\xi|}{\overline{\eta}}\right)\pi(F_-^{(0,2)} - F_-^{(0,0)}). \tag{3.22}$$

This gives us the corrected distribution of sources $\pi F_-^{(3,2)}$ in terms of an arbitrary constant $\Sigma^{(3,2)}$, this constant is determined by substituting the results into the pore pressure equation, which is

$$\frac{3\Pi_+^{(3,2)}}{2B(1+\nu_u)} = \frac{\pi B_-^{(3,2)}}{\mathrm{i}s}\frac{|\xi|}{\xi} - \frac{\pi\epsilon}{s\Gamma}(F_-^{(3,2)} + F_-^{(2,2)}). \tag{3.23}$$

The solution of this equation gives us the stress intensity factor to this order as

$$K_1(t') = \frac{\tau_0 a^{1/2}\sqrt{2}}{\overline{\eta}(-d+N_+(0)/\overline{\eta})}\left(H(t') - \frac{\mathrm{i}c_0\overline{\eta}t'^{1/4}}{N_+(0)\gamma(\frac{5}{4})}\right). \tag{3.24}$$

In a similar, but progressively more complicated manner to the above, we proceed to find higher terms in the inner and outer expansions for the dislocation and fluid source densities. This leads to the following asymptotic expression for the mode 1 stress intensity factor (in Laplace transform space).

$$\overline{K}_1(s) = \frac{\sqrt{2}\tau_0 a^{1/2}}{s\overline{\eta}(-d+N_+(0)/\overline{\eta})}(1 - (\epsilon/a^{1/2})(\epsilon^{-1}+a^{-1})^{1/2}\frac{\mathrm{i}c_0\overline{\eta}}{N_+(0)}$$
$$+ (\epsilon^2/a^{3/2})(\epsilon^{-1}+a^{-1})^{1/2}(2n_{12} - \mathrm{i}c_0\overline{\eta}(n_{11} + n_{12}\log(\epsilon/2a)))). \tag{3.25}$$

As Laplace transforms involving $(\epsilon^{-1}+a^{-1})^{1/2}$ have no simple representation after inversion into real time, we expand for small $\epsilon$ and invert to get the following real time result for $K_1(t')$,

$$K_1(t') = \frac{\sqrt{2}\tau_0 a^{1/2}}{\overline{\eta}(-d+N_+(0)/\overline{\eta})}\left(H(t') - \frac{\mathrm{i}c_0\overline{\eta}t'^{1/4}}{N_+(0)\gamma(\frac{5}{4})}\right.$$
$$\left. + \left(2n_{12} - \frac{\mathrm{i}c_0\overline{\eta}}{N_+(0)}(\tfrac{1}{2} + n_{11} + n_{12}(\log(\tfrac{1}{2}t'^{1/2}) - \tfrac{1}{2}\psi(\tfrac{7}{4})))\right)\frac{t'^{3/4}}{\gamma(\frac{7}{4})} + \cdots\right). \tag{3.26}$$

The sequence of events in the outer field is determined as follows: initially we have a loaded crack in an undrained material. To the next order a distribution of dipoles related to the elastic loading is induced along the crack faces; these are orientated to maintain the no-flow condition ahead of the crack. There is a dilatational response to these dipoles which produces a correction to the stress intensity factor at a higher order. The dipoles also induce a pore pressure along the crack faces; this is corrected for using a distribution of fluid volume sources. The asymptotic method used here corrects for each part of this in turn, bringing in the interaction terms leading to an accurate representation for the stress intensity factor in real time. The method outlined above demonstrates the asymptotic method for a system of coupled integral equations and the same method can be applied to the mixed problem considered in [CA]. The method has allowed us to separate the kernel and identify which parts of the kernel drive different responses. A graph of the exact stress intensity factor (normalized by dividing through by $\sqrt{2}\tau_0 a^{1/2}$ and for $\nu = 0.3$, $\nu_u = 0.4$) inverted numerically using the Talbot (1979) algorithm and the asymptote are shown in figure 2.

The stress intensity factor for the mixed case is less than the unmixed case, as the coefficient of singular pore pressure gradient contributes to terms in the invariant integral (4.3). We should also note that the case of a stress free crack with an internally applied pore pressure can be similarly treated. The superposition of this with the problem described in this section allows more general problems to

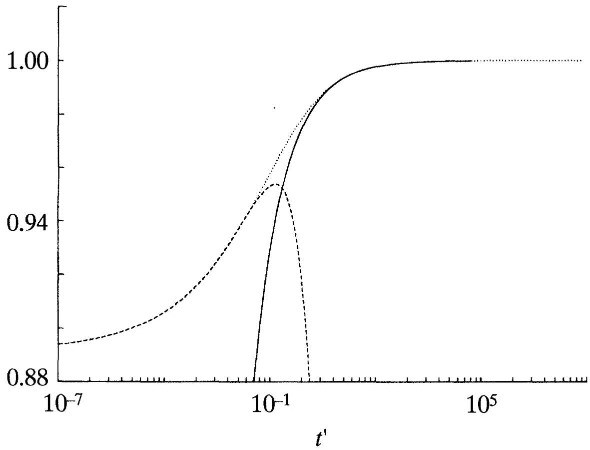


Figure 2. The non-dimensionalized mode 1 stress intensity factor (for $\nu = 0.3, \nu_{\mathrm{u}} = 0.4$) against time, for the full solution (4.15), dotted line, the small time solution, dashed line, and the large time solution, solid line.

be evaluated. The large time asymptotics are determined in a similar manner to that described for the unmixed case. This gives a large time asymptotic solution as

$$K_1(t') = \sqrt{2}\tau_0 a^{1/2}\left(H(t') + \frac{1}{\pi^{1/2}t'^{1/2}}\left(\tfrac{1}{2} + \frac{I}{\pi} + \frac{\mathrm{i}(\mathrm{i}N_+(0)/2\overline{\eta} + \varpi)}{(-d + N_+(0)/\overline{\eta})}\right)\right) + O(1/t'), \tag{3.27}$$

which is also shown in figure 2.

## 4. An invariant integral

In a previous paper (Atkinson & Craster 1992*a*, referred to as [ACa]), an invariant integral based on a 'pseudo' energy momentum tensor was introduced in the Laplace transform domain, and its use was illustrated to check the shear problem considered in [CA]. A similar check works for the tensile case as will be demonstrated in this section. By choosing an appropriate model problem we get an integral identity that acts as a powerful check on the analysis of [AC] and of this paper. The stress and pore pressure intensity factors in the mixed cases are complicated; an independent check is valuable.

By Laplace transforming the governing equations we deduce the following lagrangian as derived in Atkinson (1991) for the poroelastic equations

$$L = -\tfrac{1}{2}\overline{t}_{ij}\overline{\epsilon}_{ij} + \alpha\overline{p}\,\overline{u}_{i,i} + \frac{\kappa\overline{p}_{,i}\overline{p}_{,i}}{s} + \frac{\overline{p}^2}{2Q}. \tag{4.1}$$

The elastic stress tensor $\overline{t}_{ij}$ is defined as $\overline{\sigma}_{ij} + \alpha\overline{p}\delta_{ij}$. The Euler equations for this lagrangian recover the Laplace transformed governing equations. The lagrangian is used to derive invariant integrals based on a pseudo energy momentum tensor, $\overline{P}_{lj}$, which can be used to check various poroelastic results, as in [ACa], it is given by

$$\overline{P}_{lj} = \frac{\partial L}{\partial\overline{u}_{i,j}}\overline{u}_{i,l} + \frac{\partial L}{\partial\overline{p}_{,j}}\overline{p}_{,l} - L\delta_{lj}. \tag{4.2}$$

The invariant integral $\overline{F}_1$ defined by

$$\overline{F}_1 = \int_S \overline{P}_{1j} n_j \, \mathrm{d}S \tag{4.3}$$

is zero provided the integral encloses no singularities. The vector $n_j$ denotes the unit normal vector to $S$.

### (a) An application: the tensile problem

We now consider the problem of a permeable crack in a finite width strip subjected to symmetric pressure conditions applied at $\pm h$. We compare this in the limit as $h \to \infty$ with a pore pressure loaded fracture in an infinite material. As the method is similar to that in [ACa], we will only sketch the solution here.

Taking the semi-infinite tensile crack problem of [AC] and §3, we now consider a stress free, but pore pressure loaded fracture, i.e. on $y = 0$

$$\sigma_{22}(x, y, t) = 0, \quad p(x, y, t) = -q_0 \mathrm{e}^{x/a} H(t) \quad \text{for } x < 0, \tag{4.4}$$

ahead of the crack from symmetry we take

$$\partial p(x, y, t)/\partial y = 0, \quad u_2(x, y, t) = 0 \; x > 0, \tag{4.5}$$

and along the fracture plane we take $\sigma_{12}(x, y, t) = 0$. This problem may appear somewhat artificial, but it is convenient to decompose any loadings into a pure stress or pure pore pressure loading and then superimpose them to get the required combination. This problem works with the invariant integral; the stress free condition on the crack faces does not lead to an infinite contribution to the stress intensity factor. We take the limit as $a \to \infty$, i.e. a stress free crack, uniformly loaded by a constant pore pressure. We deduce with the full analysis from [AC] that the Laplace transformed mode 1 stress intensity factor and coefficient of the singular pore pressure gradient in this limit are given by

$$\overline{K}_1(s) = \frac{\sqrt{2}\, 3 q_0 c^{1/2} \mathrm{i} c_0 (s/c)^{1/4}}{2B(1+\nu_\mathrm{u}) s^{3/2} (d - N_+(0)/\overline{\eta}) N_+(0)}, \tag{4.6}$$

and

$$\overline{K}_2(s) = -\frac{2\sqrt{2}\, q_0 \overline{\eta} (s/c)^{1/4}}{s N_+(0)(d - N_+(0)/\overline{\eta})} \left( \left( d - \frac{N_+(0)}{\overline{\eta}} \right)^2 + c_0 \left( \frac{\mathrm{i} N_+(0)}{2\overline{\eta}} + \varpi \right) \right). \tag{4.7}$$

The appropriate constants, $c_0, d$ and $\varpi$ are given in Appendix A. The aim is to use the invariant integral to check these results.

We now turn our attention to solving the following finite width strip problem with the boundary conditions

$$\overline{u}_1 = \overline{u}_2 = 0 \text{ and } \overline{p} = p_0 f(s) \text{ on } y = \pm h, \tag{4.8}$$

and on $y = 0$

$$\overline{p} = 0 \text{ for } x < 0, \quad \partial \overline{p}/\partial y = 0 \text{ for } x > 0, \tag{4.9}$$

$$\overline{u}_2 = 0 \text{ for } x > 0, \quad \overline{\sigma}_{22} = 0 \text{ for } x < 0, \tag{4.10}$$

$$\overline{\sigma}_{12} = 0 \text{ for all } x. \tag{4.11}$$

We proceed by solving the one-dimensional governing equations at the ends of

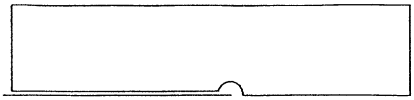

Figure 3. The contour required for the strip problem.

the strip

$$\kappa Q \frac{\mathrm{d}^2 \overline{p}}{\mathrm{d}y^2} - \alpha Q s \overline{e} - s\overline{p} = 0, \quad \overline{\sigma}_{i2,2} = 0, \tag{4.12}$$

as $x \to \pm\infty$. As in [ACa] we find the pore pressure and displacement fields along the edges of the strip. By taking the invariant integral around the contour shown in figure 3, we deduce in the limit as $h \to \infty$ that

$$\frac{\kappa \overline{K}_2^2(s)}{16s} + \frac{\overline{K}_1^2(s)(1-\nu)}{4G} = \frac{q_0^2 \kappa}{2cs^2(s/c)^{1/2}}. \tag{4.13}$$

We subtract off the field as $x \to \infty$, this problem (in the limit as $h \to \infty$) now corresponds to the uniformly loaded crack considered at the beginning of this section. Substituting in (4.6) and (4.7) gives the resulting integral identity (which is analogous to the equivalent check on the mixed, shear problem in (174) of [ACa])

$$\left(\frac{\overline{\eta}}{N_+(0)(d - N_+(0)/\overline{\eta})}\right)^2 ((d - N_+(0)/\overline{\eta})^2 + (-\mathrm{i}\varpi + N_+(0)/\overline{\eta})(\mathrm{i}c_0))^2 + \overline{\eta}\left(\frac{\mathrm{i}c_0}{(d - N_+(0)/\overline{\eta})}\right)^2 = 1, \tag{4.14}$$

the constants $d$, $c_0$ and $\varpi$ are given in Appendix A as complicated integrals involving split functions and this integral identity can now be verified numerically. This checks the intensity factors for a quite general problem and provides considerable reassurance of the accuracy of the analysis.

There is another situation which can be analysed using the invariant integral and that is to check the intensity factors in the small time limit. Let us recall the intensity factors for the mixed, tensile case which is loaded internally under an exponentially decaying tensile load, i.e. the problem considered in [AC] and § 3. The mode 1 stress intensity factor is

$$\overline{K}_1(s) = 2^{1/2}\mathrm{e}^{-\mathrm{i}\pi/4}\Sigma(s/c)^{1/4}, \quad \Sigma = \tau_0 \mathrm{i}\frac{c^{1/2}\Gamma_+(\mathrm{i}/a_1)}{s^{3/2}N_+(\mathrm{i}/a_1)}\left(\frac{(k_+(\mathrm{i}/a_1) - c_0)}{(-d + N_+(0)/\overline{\eta})}\right), \tag{4.15}$$

and the coefficient of the singular pore pressure gradient is

$$\overline{K}_2(s) = \left(\frac{c^{3/2}\tau_0\Gamma_+(\mathrm{i}/a_1)}{2G_{\mathrm{u}}s^{3/2}\kappa \mathrm{i}N_+(\mathrm{i}/a_1)}(-d + N_+(0)/\overline{\eta} + (\mathrm{i}/a_1)(c_0 - k_+(\mathrm{i}/a_1))) + \frac{c}{2G_{\mathrm{u}}\kappa}\Sigma(\mathrm{i}N_+(0)/2\overline{\eta} + \varpi)\right)\mathrm{e}^{\mathrm{i}\pi/4}(s/c)^{3/4}(2\surd 2) \tag{4.16}$$

(note that equation (86) of [AC] contains a misprint and (4.16) corrects this), the overbars denote Laplace transformed quantities and we recall that $a_1 = a(s/c)^{1/2}$. If we consider the invariant integral (4.3) in the limit as $t \to 0$ or in Laplace transform space as $s \to \infty$, we use the analysis of §3 to identify the intensity factors as an asymptotic expansion in $s$. As $s \to \infty$ we deduce the crack appears stress free (as the loading is $O(1/s)$). We apply the integral around a circular path at a distance sufficiently far from the crack tip for the material to be considered as undrained. Then we take the integral along the crack faces and around a vanishingly small circle at the crack tip. Let us take the outer solution to be the elastic crack tip solution with undrained coefficients and the inner solution to be the poroelastic crack tip solution as $s \to \infty$, i.e. from equations (3.18) and (3.19) the intensity factors are

$$\overline{K}_1(s) = \frac{\sqrt{2}\,\tau_0 a^{1/2}}{s\overline{\eta}(-d + N_+(0)/\overline{\eta})}, \tag{4.17}$$

$$\overline{K}_2(s) = \frac{\tau_0 \mathrm{i} a^{1/2}}{2G_{\mathrm{u}}\kappa\overline{\eta}}\left(\frac{\mathrm{i}N_+(0)}{2\overline{\eta}} + \varpi\right) 2\sqrt{2}\,(c/s)^{1/2}/(-d + N_+(0)/\overline{\eta}). \tag{4.18}$$

We deduce from the invariant integral that in this limit,

$$\frac{K_{\mathrm{e}}^2(1-\nu_{\mathrm{u}})}{2G} = \frac{\kappa\overline{K}_2^2(s)}{8s} + \frac{\overline{K}_1^2(s)(1-\nu)}{2G}, \tag{4.19}$$

where $K_{\mathrm{e}}$ is the stress intensity factor for a similarly loaded elastic material, i.e. $K_{\mathrm{e}} = \sqrt{2}\tau_0 a^{1/2}/s$. Equation (4.19) gives the following relation, which is checked numerically

$$\left(\frac{(1-\nu)}{(1-\nu_{\mathrm{u}})} + \overline{\eta}(N_+(0)/2\overline{\eta} - i\varpi)^2\right) = \overline{\eta}^2(-d + N_+(0)/\overline{\eta})^2. \tag{4.20}$$

This provides another valuable check on the earlier results, and another integral identity which is checked numerically. The integral invariant provides a reassuring and effective non-trivial check on the analysis both here and in [AC].

## 5. Poroelastic weight functions for cracks

Having inverted the poroelastic operators for a particular loading where the internal stress decays exponentially, it is natural to try to use the functional equations to deduce the solutions for more general loadings. Clearly, if the loading in question can be written as a sum of exponentials the stress intensity factor can be written out instantaneously. If, however, we have a point loading or a combination of more complicated loadings, this may not work. We will use the poroelastic reciprocal theorem (see, for example, Cleary 1977), which is valid provided there are no point forces or fluid sources in the body

$$\int_S \left(\overline{\sigma}_{\mathrm{i}j}\overline{u}_i^\star - \overline{\sigma}_{\mathrm{i}j}^\star\overline{u}_i + \frac{\kappa}{s}(\overline{p}\,\overline{p}_{,j}^\star - \overline{p}^\star\overline{p}_{,j})\right) n_j\,\mathrm{d}S = 0, \tag{5.1}$$

where the overbars denote Laplace transformed quantities and the $_{,j}$ denotes partial differentiation with respect to $x_j$. The starred and unstarred fields are two independent poroelastic states for the same volume $V$ with surfaces $S$, and $n_j$ is the unit normal to surface $S$. In [ACa], the reciprocal theorem was used with appropriate eigensolutions to outline a numerical method whereby far field numerical data could be used to evaluate the near crack tip fields. A similar

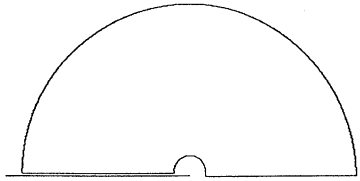

Figure 4. The contour to be used with the reciprocal theorem.

approach is used here; we choose eigensolutions of the crack problems which are too singular in the stress (or pore pressure) at the crack tip. These eigensolutions combine in the reciprocal theorem with the known asymptotic behaviour of the near crack tip fields for the 'real' problem, i.e. the stresses (and in the mixed cases, the pore pressure gradient) are square root singular, to give the integral around the crack tip in terms of the stress intensity factor. This crack tip integral is equal to an integral along the crack faces, which depends on the particular loading applied.

Let us consider the shear loaded permeable crack of § 2. Eigensolutions of this problem are deduced from (2.3) with $\tau_0 = 0$ (We set the crack face loading for our eigensolution to zero without any loss of generality). Setting $\tau_0 = 0$ also removes one of the line integrals from the reciprocal theorem. We denote our eigensolution by $^\star$ and consider stresses which are $O(r^{-3/2})$ at the crack tip, in Fourier transform space this implies that

$$\tau_+^\star \sim O(\xi_+^{1/2}) \text{ as } |\xi| \to \infty.$$

The functional equation from (2.3) is

$$\frac{\tau_+^\star}{N_+\xi_+^{1/2}} = -\frac{(2G_{\mathrm{u}})^2\kappa}{c} U_-^\star N_- \xi_-^{1/2} = C = \sqrt{2}\,\overline{K}_{\mathrm{II}}^\star(s)(s/c)^{1/4}\mathrm{i}_+^{-1/2}. \tag{5.2}$$

Remember that $\xi$ is the Fourier transform with respect to a scaled coordinate $X = x(s/c)^{1/2}$. $C$ is an arbitrary constant which is determined by Liouville's theorem and the value of $C$ is found by comparison with the known asymptotic form of the near crack tip stresses for the eigensolutions; see Appendix D. Using the reciprocal theorem along the contour shown in figure 4 and taking the limit as the outer contour tends to infinity we deduce that

$$\overline{K}_{\mathrm{II}}(s) = -\frac{1}{\mathrm{i}_+^{1/2}\sqrt{2}\,\pi}(s/c)^{1/4}\frac{(1-\nu_{\mathrm{u}})\overline{\eta}}{(1-\nu)}\int_{-\infty}^{0}\overline{\sigma}_{12}(x,0,s)\int_{-\infty}^{\infty}\frac{\mathrm{e}^{-\mathrm{i}\xi x(s/c)^{1/2}}}{N_-(\xi)\xi_-^{1/2}}\,\mathrm{d}\xi\,\mathrm{d}x. \tag{5.3}$$

We can recover the solution (2.6) for the exponentially decaying loading of § 2 using this formula. One can now consider any loading, let us choose a shear loading $\overline{\sigma}_{12}(x,0,s) = -P(s)\delta(x+l)$, i.e. a point load at $x = -l$ with arbitrary time dependence. Then we find the stress intensity factor as

$$\overline{K}_{\mathrm{II}}(s) = \frac{2^{1/2}(1-\nu_{\mathrm{u}})P(s)}{\pi(1-\nu)l^{1/2}}\left(\int_0^{l_1}\frac{\mathrm{e}^{-q}}{q^{1/2}}\frac{(1-q^2/\overline{\eta}l_1^2)}{(1-2N_+^2(0)q^2/\overline{\eta}l_1^2)}N_+(\mathrm{i}q/l_1)\,\mathrm{d}q\right.$$

$$\left.+\int_{l_1}^{\infty}\frac{\overline{\eta}\mathrm{e}^{-q}}{q^{1/2}}\frac{N_+(\mathrm{i}q/l_1)\,\mathrm{d}q}{(\overline{\eta}-(q^2/l_1^2)+q/l_1(q^2/l_1^2-1)^{1/2})}\right), \tag{5.4}$$

where $l_1 = l(s/c)^{1/2}$. In the limit as $t' \to 0$ the answer predicted by considering the crack tip to be a drained inclusion is recovered, as discussed in [CA], and as $t' \to \infty$ the elastic result is found.

The above result for the stress intensity factor (5.4) is difficult and time consuming to invert numerically and we have been unable to invert it to sufficient accuracy, beyond a small time. It is for this reason that the exponential loading has been preferred by us in previous works. Although it is simple to generalize the loading mathematically (a simple sum split in the analysis is all that is required) the numerical inversion becomes difficult; whereas, for the exponential load the sum split is not required and the inversion is more straightforward. However, by using the asymptotic procedure developed in previous sections the first three terms in the stress intensity factor (for an impulsive loading $P(s) = P/s$) are deduced as

$$\begin{aligned} K_{\text{II}}(t') \sim \frac{\sqrt{2}\,P}{N_+(0)(\pi l)^{1/2}} & (H(t') - 2(t'/\pi)^{1/2}(n_{11} - \tfrac{1}{2}n_{12}(2 - 2\log 2 - \gamma - \log t')) \\ & + t'(-(n_{21} - n_{11}^2) + (n_{11}/2\pi\overline{\eta})(1 - \gamma - \log t') \\ & + \tfrac{1}{4}n_{23}((1 - \gamma - \log t')^2 + 1 - \tfrac{1}{6}\pi^2)), \end{aligned} \tag{5.5}$$

given in terms of the non-dimensional timescale $t' = tc/4l^2$. We would expect this approximation to be as accurate as those in the previous sections. This asymptotic formula does yield some useful information; initially we have the undrained response again, after this, however, the stress intensity factor decreases slightly. The point load induces a dipole response. The subsequent fluid rearrangement initially pushes fluid towards the crack tip, leading to a volume expansion of the material, tending to close the crack in the neighbourhood of the crack tip. This is reflected by a decrease in the stress intensity factor: this is in contrast to the exponentially decaying loading for which the stress intensity factors increase monotonically. This illustrates the main application of the asymptotic procedure; it gives an accurate asymptotic expression for particular problems whose numerical solution is computationally intensive. The above inverse Laplace transform (5.4) requires in essence triple integrals to be performed which is numerically intensive; the asymptotic formula takes virtually no computer time at all. Of course it will only be accurate for small values of the non-dimensional timescale. A plot of the stress intensity factor (normalized by dividing through by the elastic result for a similarly loaded crack) is shown in figure 5 as a function of the non-dimensional timescale $t'$.

The large time asymptotics are performed in a similar manner to § 2 *b* to give

$$K_{\text{II}}(t') \sim P(2/\pi l)^{1/2}(H(t') + I/\pi^{3/2}t'^{1/2} + \cdots). \tag{5.6}$$

This is also shown in figure 5 and matches up with the small time result almost exactly.

Similar eigensolutions to those above are used to generalize the other unmixed case: the impermeable crack loaded internally under tension. The analogous formula to (5.3) for the mode 1 stress intensity factor in this case is given by

$$\overline{K}_1(s) = \frac{1}{2^{1/2}\mathrm{i}_+^{1/2}\pi}(s/c)^{1/4}\frac{(1-\nu_{\mathrm{u}})\overline{\eta}}{(1-\nu)}\int_{-\infty}^{0}\overline{\sigma}_{22}(x,0,s)\int_{-\infty}^{\infty}\frac{\mathrm{e}^{-\mathrm{i}\xi x(s/c)^{1/2}}}{\overline{N}_-(\xi)\xi_-^{1/2}}\,\mathrm{d}\xi\,\mathrm{d}x. \tag{5.7}$$





PHILOSOPHICAL TRANSACTIONS OF THE ROYAL SOCIETY A MATHEMATICAL, PHYSICAL & ENGINEERING SCIENCES

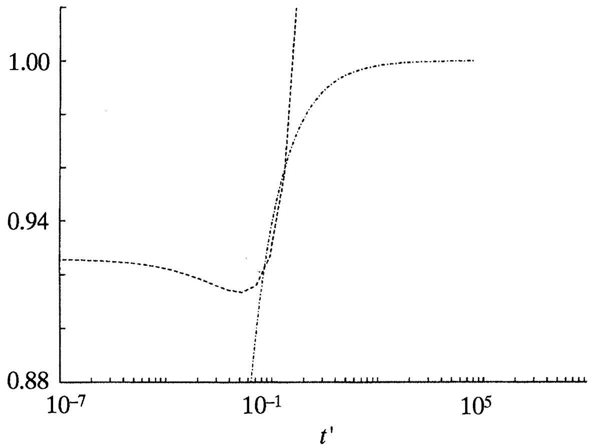


Figure 5. The non-dimensionalized mode 2 stress intensity factor (for $\nu = 0.3$, $\nu_{\mathrm{u}} = 0.4$) against time (in powers of 10) for the delta function loading, the small time solution, dashed line , and the large time solution, dot-dash line.

The mixed problems are more complicated as we now have a singular pore pressure gradient at the crack tip, hence the pore pressure gradient intensity factor will enter into the reciprocal theorem. However, it is possible to use the reciprocal theorem together with two eigensolutions to identify both intensity factors for any loading. Consider a symmetrically loaded, permeable crack, cf. § 3. We require two different eigensolutions of this problem which must combine with the asymptotic behaviour of the 'real' solution to isolate the intensity factors. The first eigensolution is too singular in both the pore pressure (i.e. $\overline{p}^{\star} \sim O(r^{-1/2})$) and the stress (i.e. $\overline{\sigma}_{22}^{\star} \sim O(r^{-3/2})$) at the crack tip. We use the reciprocal theorem to derive a relation between the sum of the intensity factors and a line integral along the crack faces

$$\frac{(1-\nu)}{G}\overline{K}_1(s)\overline{K}_1^{\star} + \frac{\kappa}{4s}\overline{K}_2(s)\overline{K}_2^{\star} = \int_{-\infty}^{0}\left(\overline{\sigma}_{22}(x,0,s)\overline{u}_2^{\star}(x,0,s) + \frac{\kappa}{s}\overline{p}(x,0,s)\frac{\partial \overline{p}^{\star}(x,0,s)}{\partial y}\right)\mathrm{d}x. \quad (5.8)$$

The other eigensolution we consider (which we denote using the superscripts ⋆⋆ to prevent confusion) is too singular in the pore pressure at the crack tip, but we take the stress to have the usual square root singularity. Because the stress eigensolution has this behaviour at the crack tip, the integral around the crack tip gives a term involving only the pore pressure gradient intensity factor, which is equal to a line integral along the crack faces

$$\frac{\kappa}{4s}\overline{K}_2(s)\overline{K}_2^{\star\star} = \int_{-\infty}^{0}\left(\overline{\sigma}_{22}(x,0,s)\overline{u}_2^{\star\star}(x,0,s) + \frac{\kappa}{s}\overline{p}(x,0,s)\frac{\partial \overline{p}^{\star\star}(x,0,s)}{\partial y}\right)\mathrm{d}x. \quad (5.9)$$

Hence, we use the two integrals to isolate the intensity factors separately. The eigensolutions required for this problem are derived in [ACa], where they are used with the reciprocal theorem to outline a possible numerical method for relating far field numerical data to near crack tip fields. We define $K_1^{\star}$ and $K_2^{\star}$ as the coefficients of the singular behaviour of the eigensolutions, i.e. in the following manner

$$\overline{p}^{\star}(r,\theta,s) \sim \frac{\overline{K}_2^{\star}}{(2\pi r)^{1/2}}\cos\tfrac{1}{2}\theta, \quad \overline{\sigma}_{ij}^{\star}(r,\theta,s) \sim \frac{\overline{K}_1^{\star}}{(2\pi r^3)^{1/2}} g_{ij}(\theta). \tag{5.10}$$

The angular variation $g_{ij}(\theta)$ is given in [ACa]. We use the results we require directly from [ACa]; for the first eigensolution

$$\overline{K}_1^{\star} = \frac{b\mathrm{i}_+^{1/2}}{\sqrt{2}}(c/s)^{1/4}, \tag{5.11}$$

$$\overline{K}_2^{\star} = -\frac{cb}{2G_{\mathrm{u}}\kappa}\left(\frac{\mathrm{i}N_+(0)}{2\overline{\eta}} + \varpi\right)(s/c)^{1/4}\frac{\sqrt{2}}{\mathrm{i}_+^{1/2}}, \tag{5.12}$$

where $b$ is an arbitrary constant. The Fourier transforms of the displacement and pore pressure gradient for the eigensolutions are also given there. By using these in (5.8), the constant $b$ cancels out and we show that

$$\begin{aligned}
&\tfrac{2}{3}B\ (1+\nu_{\mathrm{u}})\frac{(1-\nu)}{(1-\nu_{\mathrm{u}})}\overline{K}_1(s) - \tfrac{1}{2}(c/s)^{1/2}(N_+(0)/2\overline{\eta} - \mathrm{i}\varpi)\overline{K}_2(s) \\
&= \frac{(s/c)^{1/4}}{(2\mathrm{i})_+^{1/2}\pi}\int_{-\infty}^{0}\int_{-\infty}^{\infty}\Big((-\tfrac{2}{3}B(1+\nu_{\mathrm{u}})\overline{\eta}\ \overline{\sigma}_{22}(x,0,s) + \xi^2\overline{p}(x,0,s))\big(\xi(c_0+k_-(\xi)) \\
&\quad + (N_+(0)/\overline{\eta} - d)\big) - \overline{p}(x,0,s)\frac{\varGamma_-\xi_-^{3/2}}{N_-}\Big)\frac{\mathrm{e}^{-\mathrm{i}\xi x(s/c)^{1/2}}}{\xi_-^{1/2}}\,\mathrm{d}\xi\,\mathrm{d}x.
\end{aligned} \tag{5.13}$$

To isolate $\overline{K}_2(s)$ we use the second eigensolution from [ACa]. In this case the eigensolution has the usual stress singularity at the crack tip, so when this is combined with the asymptotic behaviour of the loaded crack this gives no contribution to the reciprocal theorem. In this case

$$\overline{K}_2^{\star\star} = \frac{ac}{2G_{\mathrm{u}}\kappa}\frac{\sqrt{2}}{\mathrm{i}_+^{1/2}}(N_+(0)/\overline{\eta} - d)(s/c)^{1/4}, \tag{5.14}$$

where $a$ is an arbitrary constant which cancels out later in the analysis. The Fourier transforms of the displacement and pore pressure gradient follow from results in [ACa], hence it is deduced that

$$\begin{aligned}
\overline{K}_2(s) = \frac{1}{\pi}\int_{-\infty}^{0}\int_{-\infty}^{\infty}&((-\tfrac{2}{3}B(1+\nu_{\mathrm{u}})\overline{\eta}\ \overline{\sigma}_{22}(x,0,s) + \xi^2\overline{p}(x,0,s))\frac{(k_- + c_0)}{\xi_-^{1/2}} \\
&- \overline{p}(x,0,s)\frac{\varGamma_-}{N_-})\frac{\mathrm{e}^{-\mathrm{i}\xi x(s/c)^{1/2}}(s/c)^{3/4}\mathrm{i}_+^{1/2}\sqrt{2}}{(N_+(0)/\overline{\eta} - d)}\,\mathrm{d}\xi\,\mathrm{d}x.
\end{aligned} \tag{5.15}$$

These results can be checked for the spatially exponentially decaying stress or pore pressure loaded crack considered in [AC]. The integral indentity (A 27) from Appendix A is required, and the formulae above generalize the results for the intensity factors (4.15) and (4.16) to a completely arbitrary loading.

By using appropriate eigensolutions the mixed, anti-symmetric problem considered in [CA] can be similarly generalized. The method above demonstrates how the reciprocal theorem can be used together with eigensolutions of functional equations to generalize the results with little effort.

Such generalizations have been used to derive the weight functions for elastostatic problems (see, for example, Rice 1972) and a method closer to that used here has been used by Burridge (1976) for elastodynamic problems. Once the operators for any particular system have been inverted this can be utilized via the reciprocal theorem to extend the range of the results.

## 6. Conclusion

In this paper we have re-examined the semi-infinite crack problems in an undamaged poroelastic material. The following are the main results.

1. The crack problems are reformulated as integral equations using distibutions of dislocations (and fluid sources where appropriate). We have been able to uncouple (for small times) the problems partly. This allows an asymptotic procedure to be set up to solve these problems for small times and allows the physical processes that drive the intensity factors to be interpreted.

2. The stress intensity factors for the crack problems loaded internally with an impulsively applied and spatially exponentially decaying load, are found as an asymptotic expansion for small times. This is an improvement on the previous analysis, which relied on numerical inversion of Laplace transforms. The above asymptotic method can be utilised to provide real time approximations for the stress intensity factors for any loading and this is illustrated by considering a point loaded crack. The asymptotic method, now its accuracy has been verified, can also be applied to more complicated crack or inclusion problems to obtain accurate, concise, real time results. In Atkinson & Craster (1993) some of the integral equations that occur for finite length cracks are solved using singular perturbation methods that are related to the method used here.

3. A large-time method is also derived and utilized to derive asymptotic large-time formulae for the stress intensity factors.

4. The reciprocal theorem is used together with eigensolutions of the crack problems to generate formulae that give the stress intensity (or pore pressure gradient intensity where necessary) factors for any internal loading.

5. An invariant integral is used to check one of the more complicated problems: the tensile case with mixed pore pressure boundary conditions on the fracture plane, in two different situations.

C. A. thanks the Royal Society/SERC Industrial Fellowship scheme for their support and R.C. the SERC for a Research Studentship. R. C. also thanks Corpus Christi College, Cambridge for a Research Fellowship. Part of this work was done while both of us were at Schlumberger Cambridge Research and the computing and other facilities of Schlumberger Cambridge Research are gratefully acknowledged. We thank a referee for helpful suggestions.

## Appendix A. Fourier transforms

If $F$ denotes the Fourier transform operator, then

$$F^{-1}\left(\frac{1}{\xi_+^{n+1/2}}\right) = \frac{x^{n-1/2}H(x)}{\mathrm{i}_+^{n+1/2}\gamma(n+1/2)}, \tag{A 1}$$





PHILOSOPHICAL TRANSACTIONS OF THE ROYAL SOCIETY A MATHEMATICAL, PHYSICAL & ENGINEERING SCIENCES

where $n$ is an integer, $\gamma(z)$ is the Gamma function defined to be

$$\gamma(n+1)=\int_0^\infty t^n \mathrm{e}^{-t}\,\mathrm{d}t. \tag{A 2}$$

For the displacement fields the following transforms have to be inverted,

$$F^{-1}\left(\frac{\mathrm{e}^{-|\xi|y}}{|\xi|}\right)=-\frac{1}{\pi}\log(r),\quad F^{-1}\left(\frac{\mathrm{e}^{-|\xi|y}}{\xi}\right)=\frac{\mathrm{i}}{\pi}\arctan\left(\frac{y}{x}\right)=\frac{\mathrm{i}\theta}{\pi}. \tag{A 3}$$

These are arbitrary up to a constant, but because the displacements are similarly arbitrary this constant is taken to be zero. If we let $\Gamma^2=\xi^2+a^2$ we similarly deduce that

$$F^{-1}\left(\mathrm{e}^{-\Gamma y}\right)=\frac{ay}{\pi r}K_1(ar),\quad F^{-1}\left(\frac{\mathrm{e}^{-\Gamma y}}{\Gamma}\right)=\frac{1}{\pi}K_0(ar). \tag{A 4}$$

In the text we also use the inverse Fourier transform of the delta function, $F^{-1}(1)=\delta(x)$. Using these basic transform results we can generate the inverse transforms of $\xi f(\xi)$ and $\Gamma f(\xi)$ by partial differentiation with respect to $x$ and $y$ respectively. The outer solutions to the integral equations contain terms that include

$$F^{-1}\left(\frac{1}{\xi_+^{n+1/2}}\log(\xi/2\mathrm{i})\right)=\frac{x^{n-1/2}H(x)}{\mathrm{i}_+^{n+1/2}\gamma(n+\frac{1}{2})}(\psi(\tfrac{1}{2}-n)-\log(2x)), \tag{A 5}$$

$$F^{-1}\left(\frac{1}{\xi_+^{n+1/2}}(\log(\xi/2\mathrm{i}))^2\right)=\frac{x^{n-1/2}H(x)}{\mathrm{i}_+^{n+1/2}\gamma(n+\frac{1}{2})}(-\pi^2+(\psi(\tfrac{1}{2}-n)-\log(2x))^2 -\zeta(2,\tfrac{1}{2}-n)), \tag{A 6}$$

where $\zeta(2,\nu)$ is Riemann's generalized zeta function. To invert the Laplace Transforms for the dislocation solutions we use 29.3.122 of Abramowitz & Stegun (1970, hereafter [A]), i.e.

$$L^{-1}(s^{-1/2}K_1(ks^{1/2}))=k^{-1}\mathrm{e}^{-k^2/4t}, \tag{A 7}$$

and 29.3.120 together with the convolution theorem to deduce that

$$L^{-1}(s^{-1}K_0(ks^{1/2}))=\tfrac{1}{2}E_1(k^2/4t),\quad L^{-1}(s^{-3/2}K_1(ks^{1/2}))=(t/k)E_2(k^2/4t)). \tag{A 8}$$

The $E_{\mathrm{i}}$ above are exponential integrals ([A] 5.1.4). Below the symbol $\gamma$ (with no argument) is used to denote Euler's constant and the digamma function $\psi(k)$ used in the inverse Laplace transform results below is described in 6.3 of [A],

$$L^{-1}((\log s)/s^k)=\frac{t^{k-1}}{\gamma(k)}(\psi(k)-\log t),$$

$$L^{-1}((\log s)^2/s^k)=\frac{t^{k-1}}{\gamma(k)}((\psi(k)-\log t)^2-\psi'(k)). \tag{A 9}$$

Dawson's integral $D(x)$ and a function defined as $D_l(x)$ used in the text are given by

$$D(x)=\mathrm{e}^{-x^2}\int_0^x \mathrm{e}^{t^2}\,\mathrm{d}t,\quad D_l(x)=\mathrm{e}^{-x^2}\int_0^x \mathrm{e}^{t^2}(\psi(\tfrac{1}{2})-2\log t)\,\mathrm{d}t. \tag{A 10}$$

Fourier transforms involving $D(x)$ are derived in [AC] and [CA].

For the product splits required in the text we define $N(\xi)$ as

$$N(\xi) = \xi^2 - |\xi|(\xi^2+1)^{1/2} + \overline{\eta}. \tag{A 11}$$

From contour integration as in [AC] we find

$$\log\left(-\frac{N_-(\xi)}{N_0}\right) = -\frac{1}{\pi}\int_0^1 \arctan\left(\frac{p(1-p^2)^{1/2}}{p^2-\overline{\eta}}\right)\frac{\mathrm{d}p}{p+\mathrm{i}\xi}. \tag{A 12}$$

Although initially defined in the lower half plane, by analytic continuation this defines a function valid in the whole complex plane except for the branch cut $\mathrm{i}0_+$ to i. The 'plus' function is given from this by $N_+(\xi) = -N_-(-\xi)/N_0)$. This result is used to show that

$$N_+(0) = ((1-\nu)/(1-\nu_\mathrm{u}))^{1/2}.$$

In the text we require the asymptotic behaviour of $N_+(\xi)$ as $\xi \to 0$, it is easy to rewrite $\log N(\xi)$ as $\log N(\xi) = \log N_+(\xi) + \log N_-(\xi)$. By differentiating $\log N(\xi)$ and after some manipulation an alternative representation of $N_+(\xi)$ is found as

$$N_+(\xi) = N_+(0)\left(1+\frac{\mathrm{i}\xi}{(\frac{1}{2}\overline{\eta})^{1/2}N_+(0)}\right)^{\pi^{-1}\arctan\mu}\left(1-\frac{\mathrm{i}\xi}{(\frac{1}{2}\overline{\eta})^{1/2}N_+(0)}\right)^{\pi^{-1}\operatorname{arccot}\mu}$$

$$\times\exp\left[\frac{\mathrm{i}}{\pi}\int_0^\xi \frac{\xi^2+\frac{1}{2}N_+^2(0)}{\xi^2+\frac{1}{2}\overline{\eta}N_+^2(0)}\log\left(\frac{(1+\xi^2)^{1/2}+1-\mathrm{i}\xi}{1-(1+\xi^2)^{1/2}-\mathrm{i}\xi}\right)\frac{\mathrm{d}\xi}{(1+\xi^2)^{1/2}}\right], \tag{A 13}$$

where

$$\mu = \left(\frac{(\frac{1}{2}\overline{\eta}N_+^2(0)-1)^{1/2}}{(\frac{1}{2}\overline{\eta})^{1/2}N_+(0)+1}\right).$$

The branch points here would initially appear to contradict the definition of $N_+$ as a 'plus' function, but they do in fact cancel with terms in the integral. This expression is checked numerically against $N_+$ as defined by collapsing the contour integral around the branch cuts. The exponential term in (A 13) can be rewritten in a form more convenient for numerical work as

$$\exp\left[\frac{1}{\pi}\int_0^{\arcsin(\xi/\mathrm{i})}\frac{\frac{1}{2}N_+(0)^2-\sin^2\theta}{\frac{1}{2}\overline{\eta}N_+(0)^2-\sin^2\theta}\log(\tan\tfrac{1}{2}\theta)\,\mathrm{d}\theta\right]. \tag{A 14}$$

The alternative expression for $N_+(\xi)$ is of value as from (A 13) we find an asymptotic expansion for $N_+(\xi)$ for $\xi$ small as

$$\begin{aligned}\frac{N_+(\xi)}{N_+(0)} &= 1 - \frac{\mathrm{i}\xi}{\pi\overline{\eta}}\log(\xi/2\mathrm{i}) + \frac{\mathrm{i}\xi}{\pi\overline{\eta}} + \frac{\xi^2}{\pi^2\overline{\eta}^2}\log(\xi/2\mathrm{i}) - \frac{\xi^2}{2\pi^2\overline{\eta}^2}\\ &\quad -\frac{\xi^2}{2\pi^2\overline{\eta}^2}\log^2(\xi/2\mathrm{i}) - \frac{\mathrm{i}\xi\operatorname{arccot}((\frac{1}{2}\overline{\eta}N_+^2(0)-1)^{1/2})}{(\frac{1}{2}\overline{\eta})^{1/2}N_+(0)\pi}\\ &\quad -\frac{\xi^2\log(\xi/2\mathrm{i})\operatorname{arccot}((\frac{1}{2}\overline{\eta}N_+^2(0)-1)^{1/2})}{\pi^2\overline{\eta}(\frac{1}{2}\overline{\eta})^{1/2}N_+(0)} + \frac{\xi^2\operatorname{arccot}((\frac{1}{2}\overline{\eta}N_+^2(0)-1)^{1/2})}{\pi^2\overline{\eta}(\frac{1}{2}\overline{\eta})^{1/2}N_+(0)}\\ &\quad -\frac{\xi^2}{\overline{\eta}N_+^2(0)}\left(\frac{1}{\pi^2}(\operatorname{arccot}((\tfrac{1}{2}\overline{\eta}N_+^2(0)-1)^{1/2}))^2-\tfrac{1}{2}\right)+O(\xi^3).\end{aligned} \tag{A 15}$$

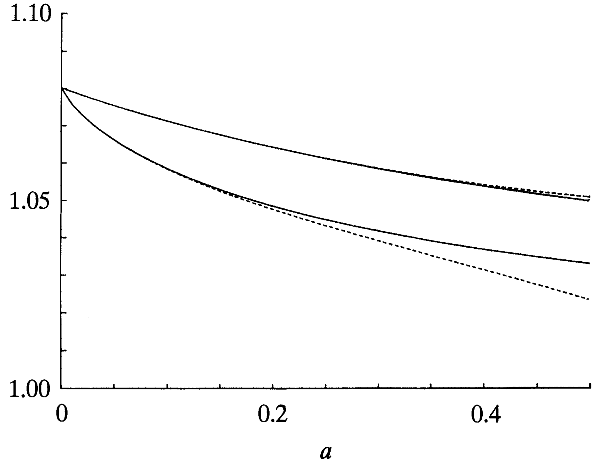


Figure 6. A comparison of the exact (solid) and asymptotic (dashed) values of $N_+(ia), \overline{N}_+(ia)$ for $\overline{\eta} = 3.5$. The upper pair of lines are those for $\overline{N}_+(ia)$ and the lower pair for $N_+(ia)$.

For convenience we will write this asymptotic expansion as

$$N_+(\xi) = N_+(0)(1 + \mathrm{i}\xi(n_{11} + n_{12}\log(\xi/2\mathrm{i})) - \xi^2(n_{21} + n_{22}\log(\xi/2\mathrm{i}) + n_{23}(\log(\xi/2\mathrm{i}))^2) + \cdots. \quad \text{(A 16)}$$

To show the accuracy of this a graph of $N_+(\mathrm{i}a)$ for real $a$ and the series approximation for $N_+(\mathrm{i}a)$ in figure 6.

Although we present this graph for imaginary $\xi$ only, a similar accuracy is obtained along other rays from the origin. This suggests we have successfully captured the essential behaviour of $N_+(\xi)$ in the neighbourhood of the origin.

There is a simple relation between the coefficients in (A 16)

$$n_{21} = \tfrac{1}{2}n_{11}^2 - (2\overline{\eta}N_+^2(0))^{-1}, \quad n_{23} = \tfrac{1}{2}n_{12}^2, \quad n_{22} = n_{12}n_{11}. \quad \text{(A 17)}$$

The sum split term $k(\xi)$ in [AC] is given by

$$k_+(\xi) + k_-(\xi) = \frac{1}{N_-(\xi)\Gamma_+(\xi)\xi_+^{1/2}}. \quad \text{(A 18)}$$

We note here in the sum split of $k(\xi)$ in [AC] there is a error in (197), which should read

$$\frac{1}{2\pi\mathrm{i}}\int_C \frac{K(z)}{z-\xi}\,\mathrm{d}z = \frac{1}{\pi}\int_0^1 \frac{\mathrm{d}y}{(\mathrm{i}y+\xi)y^{1/2}(1-y)^{1/2}}\left(\frac{1}{N_-(-\mathrm{i}y)} - \frac{N_+(0)}{\overline{\eta}}\right). \quad \text{(A 19)}$$

The asymptotic behaviour of this function is given in [AC] as $|\xi| \to \infty$

$$k_+ \to c_0 + (N_+(0)/\overline{\eta} - d)\xi^{-1} - (\mathrm{i}N_+(0)/2\overline{\eta} + \varpi)\xi^{-2} + \cdots \quad \text{(A 20)}$$

and

$$k_- \to -c_0 + (d - N_0^{-1} - N_+(0)/\overline{\eta})\xi^{-1} + \left(\varpi + \tfrac{1}{2}\mathrm{i}\left(\frac{N_+(0)}{\overline{\eta}} + \frac{1}{N_0} + \frac{I}{N_0}\right)\right)\xi^{-2} + \cdots, \quad \text{(A 21)}$$

where the constants are

$$I = \frac{2}{\pi}\int_0^1 \arctan\left(\frac{p(1-p^2)^{1/2}}{p^2-\overline{\eta}}\right) \mathrm{d}p, \tag{A 22}$$

$$c_0 = -\frac{1}{\mathrm{i}\pi}\int_0^1 \frac{\mathrm{d}y}{y^{3/2}(1-y)^{1/2}}\left(\frac{1}{N_-(-iy)} - \frac{N_+(0)}{\overline{\eta}}\right), \tag{A 23}$$

$$d = -\frac{1}{\pi}\int_0^1 \frac{\mathrm{d}y}{y^{1/2}(1-y)^{1/2}}\left(\frac{1}{N_-(-iy)} - \frac{N_+(0)}{\overline{\eta}}\right), \tag{A 24}$$

$$\varpi = \frac{\mathrm{i}}{\pi}\int_0^1 \frac{y^{1/2}\,\mathrm{d}y}{(1-y)^{1/2}}\left(\frac{1}{N_-(-iy)} - \frac{N_+(0)}{\overline{\eta}}\right). \tag{A 25}$$

An alternative expression for $k_-$ is found explicitly as

$$\mathrm{i}(k_-(\xi)+c_0) = -\frac{1}{\pi}\int_0^1 \frac{p^{1/2}(1-p)^{1/2}N_+(\mathrm{i}p)}{(p+\mathrm{i}\xi)(p^2(1-2\overline{\eta})+\overline{\eta}^2)}\,\mathrm{d}p. \tag{A 26}$$

By using these results, together with the reciprocal theorem, we deduce the integral identity

$$\begin{aligned}
&\overline{\eta}\ \left((-\mathrm{i}/a_1)(c_0+k_-(-\mathrm{i}/a_1)) + (N_+(0)/\overline{\eta}-d)\right)\\
&\quad= \frac{(1+a_1^{-1})^{1/2}}{a_1^{1/2}N_+(\mathrm{i}/a_1)}\left(\frac{(1-\nu)}{(1-\nu_{\mathrm{u}})}\frac{\mathrm{i}(k_+(\mathrm{i}/a_1)-c_0)}{(N_+(0)/\overline{\eta}-d)} + \overline{\eta}\left(\frac{N_+(0)}{2\overline{\eta}} - \mathrm{i}\varpi\right)\right.\\
&\quad\times\Big( -\left(N_+(0)/\overline{\eta}-d\right) + (\mathrm{i}/a_1)(c_0 - k_+(\mathrm{i}/a_1))\Big)\\
&\qquad\left. +(N_+(0)/2\overline{\eta}-\mathrm{i}\varpi)\frac{\mathrm{i}(k_+(\mathrm{i}/a_1)-c_0)}{(N_+(0)/\overline{\eta}-d)}\Big)\right).
\end{aligned} \tag{A 27}$$

This can be verified numerically, other integral relations can be similarly found. The asymptotic behaviour of $k_+(\xi)$ as $\xi \to 0$ be deduced as

$$k_+(\xi) \sim \frac{N_+(\xi)}{\overline{\eta}\Gamma_+(\xi)\xi_+^{1/2}} - \frac{N_+(0)}{\overline{\eta}\Gamma_+\xi_+^{1/2}}\frac{\mathrm{i}\xi n_{12}}{\pi}\log\left(\frac{\Gamma_+ + \xi_+^{1/2}}{\Gamma_+ - \xi_+^{1/2}}\right) + O(\xi). \tag{A 28}$$

The following sum split has been utilised, together with the asymptotic representation for $N_+(\xi)$,

$$\left(\frac{1}{\Gamma_+\xi_-^{1/2}}\right)_+ = \frac{1}{\Gamma_+\xi_+^{1/2}}\frac{\mathrm{i}}{\pi}\log\left(\frac{\Gamma_+ + \xi_+^{1/2}}{\Gamma_+ - \xi_+ d^{1/2}}\right). \tag{A 29}$$

For the impermeable kernel function $\overline{N}(\xi)$, which is defined as

$$\overline{N}(\xi) = (\xi^2/\Gamma)(\Gamma - |\xi|) - \overline{\eta}, \tag{A 30}$$

we perform a similar analysis to that done for $N(\xi)$. We note that $\overline{N}(\xi)$ has zeros in the cut plane at $\xi = \pm\mathrm{i}\alpha_1$, where $\alpha_1$ is given by

$$\alpha_1 = \left(\overline{\eta}\frac{(2-\overline{\eta}) + (\overline{\eta}^2+4\overline{\eta})^{1/2}}{2(2\overline{\eta}-1)}\right)^{1/2}. \tag{A 31}$$





PHILOSOPHICAL TRANSACTIONS OF THE ROYAL SOCIETY A MATHEMATICAL, PHYSICAL & ENGINEERING SCIENCES

We deduce that $\overline{N}(\xi)$ has branch cuts from $\mathrm{i}0_\pm$ to $\pm\mathrm{i}\alpha_1$. In [CA] it is shown that

$$\log\left(\frac{\overline{N}_-(\xi)}{N_0}\right)=\frac{1}{\pi}\int_0^1 \arctan\left(\frac{p^3}{(p^2+\overline{\eta})(1-p^2)^{1/2}}\right)\frac{\mathrm{d}p}{p+\mathrm{i}\xi}+\log\left(\frac{\alpha_1+\mathrm{i}\xi}{1+\mathrm{i}\xi}\right). \tag{A 32}$$

Although initially defined in the lower half plane, by analytic continuation this defines a function valid in the whole complex plane, except for the branch cut from $\mathrm{i}0_+$ to $\mathrm{i}\alpha_1$.

The result for $\overline{N}_+(\xi)$ is the complex conjugate of $\overline{N}_-(\xi)/N_0$. Note that

$$\overline{N}_+(0)=N_+(0)=\left(\frac{1-\nu}{1-\nu_\mathrm{u}}\right)^{1/2}.$$

This is checked numerically in both [CA] and [AC], and in [CA] is used in the asymptotic limit as $t\to 0$ to prove in the unmixed cases that the stress intensity factors are the same as those for a crack tip embedded in a drained inclusion.

As with (A 13) above we deduce another expression for $\overline{N}_+(\xi)$ as

$$\begin{aligned}\overline{N}_+(\xi)=\ &\frac{\overline{N}_+(0)(\alpha_1-\mathrm{i}\xi)}{\alpha_1(1-\mathrm{i}\xi)^{1/2}}\left(1+\frac{\mathrm{i}\xi}{\alpha_-^{1/2}}\right)^{-\pi^{-1}\arctan\vartheta}\left(1-\frac{\mathrm{i}\xi}{\alpha_-^{1/2}}\right)^{-\pi^{-1}\operatorname{arccot}\vartheta}\\ &\times\left(1+\frac{\xi}{(-\alpha_+)^{1/2}}\right)^{\frac14+\varphi}\left(1-\frac{\xi}{(-\alpha_+)^{1/2}}\right)^{\frac14-\varphi}\\ &\times\exp\left[\frac{1}{\pi}\int_0^{\arcsin(\xi/\mathrm{i})}\frac{\sin^2\phi(\sin^2\phi+3\overline{\eta}/(1-2\overline{\eta}))}{(\alpha_+-\sin^2\phi)(\alpha_--\sin^2\phi)}\log(\tan\tfrac12\phi)\,\mathrm{d}\phi\right]\end{aligned} \tag{A 33}$$

where

$$\vartheta=\left(\frac{(\alpha_--1)^{1/2}}{\alpha_-^{1/2}+1}\right),\qquad \varphi=\frac{\mathrm{i}}{2\pi}\log\left(\frac{(-\alpha_+)^{1/2}}{(1-\alpha_+)^{1/2}-1}\right);$$

with

$$\alpha_\pm=\left(\overline{\eta}\frac{(\overline{\eta}-2)\pm(\overline{\eta}^2+4\overline{\eta})^{1/2}}{2(1-2\overline{\eta})}\right). \tag{A 34}$$

The following asymptotic series for $\overline{N}_+(\xi)$ for $\xi$ small is deduced

$$\begin{aligned}\overline{N}_+(\xi)\sim\overline{N}_+(0)(1&+\xi(c_1+d_1)+\xi^2(c_2+c_1d_1+d_2)\\ &+\xi^3(c_3+c_1d_2+c_2d_1+d_3-\tfrac13 e_3)+\xi^3e_3\log(\xi/2\mathrm{i})).\end{aligned} \tag{A 35}$$

The coefficients are given by

$$a_1=\frac{\mathrm{i}}{\pi\alpha_-^{1/2}}\operatorname{arccot}(\alpha_--1)^{1/2},\quad a_2=\tfrac12(a_1^2-1/2\alpha_-),\quad a_3=a_1(\tfrac13 a_2-1/2\alpha_-), \tag{A 36}$$

$$\left.\begin{aligned}b_1&=(\mathrm{i}/\pi(-\alpha_+)^{1/2})\log[(-\alpha_+)^{1/2}/((1-\alpha_+)^{1/2}-1)],\\ b_2&=\tfrac12(b_1^2+1/2\alpha_+),\quad b_3=\tfrac13 b_1(b_2-1/2\alpha_+),\end{aligned}\right\} \tag{A 37}$$

$$d_1=a_1+b_1,\quad d_2=b_2+a_1b_1+a_2,\quad d_3=b_3+a_1b_2+a_2b_1+a_3, \tag{A 38}$$

$$c_1=\mathrm{i}(\tfrac12-\alpha_1^{-1}),\quad c_2=(\tfrac12\alpha_1^{-1}-\tfrac38),\quad c_3=\tfrac{1}{16}\mathrm{i}(6\alpha_1^{-1}-5), \tag{A 39}$$

$$e_3 = \mathrm{i}/\pi\overline{\eta}. \tag{A 40}$$

Equation (A 35) can be written as

$$\overline{N}_+(\xi) \sim \overline{N}_+(0)\left(1 + \mathrm{i}\xi\overline{n}_1 + \xi^2\overline{n}_2 + \xi^3(\overline{n}_3 + \overline{n}_{31}\log(\xi/2\mathrm{i})) + \cdots\right), \tag{A 41}$$

where, in particular, $2\overline{n}_2 = -\overline{n}_1^2 - 1/\overline{\eta}$. Note this expression contains no logarithmic terms until order $\xi^3$, implying the explicit diffusion interaction occurs at a later stage in the equations. A graph of the series (A 35) is shown in figure 6 together with the exact result for $\overline{N}_+(\mathrm{i}a)$. This expansion is more accurate in relative terms than (A 16) as we have taken the expansion to a higher order.

## Appendix B. The Fourier transformed variables

These representations for the Fourier transformed displacements, stresses and pore pressure (in unscaled variables) are taken from Craster & Atkinson (1992*b*)

$$u_1 = -\mathrm{i}\chi\left(A_1(\chi)\mathrm{e}^{-|\chi|y} + A_2(\chi)\mathrm{e}^{-\Gamma y} + yB_1(\chi)\mathrm{e}^{-|\chi|y}\right), \tag{B 1}$$

$$u_2 = -|\chi|A_1(\chi)\mathrm{e}^{-|\chi|y} - \Gamma A_2(\chi)\mathrm{e}^{-\Gamma y} - yB_1(\chi)|\chi|\mathrm{e}^{-|\chi|y} - (3-4\nu_\mathrm{u})B_1(\chi)\mathrm{e}^{-|\chi|y}, \tag{B 2}$$

$$p = \frac{2G\eta}{\alpha}(\Gamma^2 - \chi^2)A_2(\chi)\mathrm{e}^{-\Gamma y} - 2\alpha Q(1-2\nu_\mathrm{u})|\chi|B_1(\chi)\mathrm{e}^{-|\chi|y}, \tag{B 3}$$

$$\sigma_{12} = 2G\mathrm{i}\chi(A_1(\chi)|\chi|\mathrm{e}^{-|\chi|y} + \Gamma A_2(\chi)\mathrm{e}^{-\Gamma y} + y|\chi|B_1(\chi)\mathrm{e}^{-|\chi|y} + (1-2\nu_\mathrm{u})B_1(\chi)\mathrm{e}^{-|\chi|y}), \tag{B 4}$$

$$\sigma_{22} = 2G(\chi^2(A_1(\chi)\mathrm{e}^{-|\chi|y} + A_2(\chi)\mathrm{e}^{-\Gamma y}) + 2(1-\nu_\mathrm{u})|\chi|B_1(\chi)\mathrm{e}^{-|\chi|y} + y\chi^2B_1(\chi)\mathrm{e}^{-|\chi|y}), \tag{B 5}$$

$$\sigma_{11} = 2G(-y\chi^2B_1(\chi)\mathrm{e}^{-|\chi|y} - (\chi^2A_1(\chi)\mathrm{e}^{-|\chi|y} + \Gamma^2A_2(\chi)\mathrm{e}^{-\Gamma y}) + 2\nu_\mathrm{u}|\chi|B_1(\chi)\mathrm{e}^{-|\chi|y}). \tag{B 6}$$

## Appendix C. Dislocation solutions

In this appendix we list the dislocation solutions for a poroelastic material that are unmixed in the pore pressure boundary condition on the glide or opening plane. The jump in displacement for the shear dislocations is taken to be

$$[u_1]_{y=0_-}^{y=0_+} = \frac{2b(1-\nu_\mathrm{u})}{G}\pi H(t)H(-x), \tag{C 1}$$

with a similar representation for the tensile dislocation with $u_1$ replaced by $u_2$. These solutions can be deduced rapidly from the potentials in Appendix 2 and transform results in Appendix 1 above. The unmixed cases are well known and can be deduced from the complex variable approach of [RC] or alternatively by noticing that the fluid response and elastic responses uncouple as in Detournay & Cheng (1987). In particular the unmixed dislocations can be shown to be identical to an elastic dislocation with a dipole at the end of the dislocation orientated to maintain the pore pressure boundary condition. Note we do not consider dislocations that would have discontinuous pore pressure or pore pressure gradients ahead of the dislocation. These have been treated by Rudnicki (1987) in the context of the re-fracturing of a pre-existing geological fault whose faces have becomes blocked by clay. These solutions are not applicable to the fracture of 'virgin' rock so we do not consider them here. These solutions can also be derived using the potentials; however, the transforms are often more awkward to invert for these cases.

Below a double overbar denotes both Fourier and Laplace transformed quantities, a single overbar denotes Laplace transformed quantities and no overbar gives the field variable in real time and space. The inverse Fourier and Laplace transforms required are given in Appendix A above. In our applications above we work directly with integral equations deduced from a distribution of displacement or pore pressure dislocations.

When evaluating the inverse transforms associated with the dislocations there is no advantage in working in the scaled variables. There is no convenient length scale to non-dimensionalize with, so we write

$$\Gamma^2 = \chi^2 + s/c, \tag{C 2}$$

in the following expressions. The functions $\Gamma_{\mp}$ below are now taken to be $(\chi \mp \mathrm{i}(s/c)^{1/2})^{1/2}$ with branch cuts taken from $\pm\mathrm{i}(s/c)^{1/2}$ to $\pm\mathrm{i}\infty$. As in the text we take $\epsilon$ below to be defined as $\epsilon = (c/s)^{1/2}$.

We also note that we have considered the Heaviside step function $H(-x)$ to be the limit as $d \to 0$ in the function $\mathrm{e}^{dx}$ for $x < 0$, $0$ for $x \geqslant 0$. Hence, we take the Fourier transform of $H(-x)$ to be $1/(\mathrm{i}\chi)$ and take it as a minus function where necessary.

### (a) The gliding (shear) dislocation with permeable faces

$$\bar{\bar{p}} = -\frac{2B(1+\nu_{\mathrm{u}})\pi b}{3s}(\mathrm{e}^{-\Gamma y} - \mathrm{e}^{-|\chi|y}), \tag{C 3}$$

$$\bar{p} = -\frac{2B(1+\nu_{\mathrm{u}})b}{3s}\left(\frac{y}{r\epsilon}K_1(r/\epsilon) - \frac{y}{r^2}\right), \tag{C 4}$$

$$p = \frac{2B(1+\nu_{\mathrm{u}})b}{3}\frac{y}{r^2}\left(H(t) - \mathrm{e}^{-r^2/4ct}\right), \tag{C 5}$$

$$\bar{\bar{u}}_1 = -\frac{\pi b i}{2Gs}\left(\frac{\chi\epsilon^2}{\eta}(\mathrm{e}^{-|\chi|y} - \mathrm{e}^{-\Gamma y}) - \frac{y\chi}{|\chi|}\mathrm{e}^{-|\chi|y} + \frac{2(1-\nu_{\mathrm{u}})}{\chi}\mathrm{e}^{-|\chi|y}\right), \tag{C 6}$$

$$\bar{u}_1 = \frac{b}{Gs}\left(\frac{xy}{2r^2} + (1-\nu_{\mathrm{u}})\theta + \frac{y\epsilon}{\eta}\left(-\frac{x\epsilon}{r^2} + \frac{x}{r^3}K_1(r/\epsilon) + \frac{1}{2\epsilon}K_0(r/\epsilon)\right)\right), \tag{C 7}$$

$$u_1 = \frac{b}{G}\left(\left(\frac{xy}{2r^2} + (1-\nu_{\mathrm{u}})\theta\right)H(t) + \frac{xyct}{\eta r^4}(\mathrm{e}^{-\frac{r^2}{4ct}} - 1)\right), \tag{C 8}$$

$$\bar{\bar{u}}_2 = \frac{\pi b}{2Gs}\left(\frac{\epsilon^2}{\eta}(\Gamma\mathrm{e}^{-\Gamma y} - |\chi|\mathrm{e}^{-|\chi|y}) + y\mathrm{e}^{-|\chi|y} + \frac{(1-2\nu_{\mathrm{u}})}{|\chi|}\mathrm{e}^{-|\chi|y}\right), \tag{C 9}$$

$$\bar{u}_2 = \frac{b}{2Gs}\left(\frac{y^2}{r^2} - (1-2\nu_{\mathrm{u}})\log r + \frac{\epsilon}{\eta}\left(\frac{(x^2-y^2)\epsilon}{r^4} - \frac{(x^2-y^2)}{r^3}K_1(r/\epsilon) + \frac{y^2}{r^2\epsilon}K_0(r/\epsilon)\right)\right), \tag{C 10}$$





PHILOSOPHICAL TRANSACTIONS OF THE ROYAL SOCIETY A MATHEMATICAL, PHYSICAL & ENGINEERING SCIENCES

$$u_2 = \frac{b}{2G}\left( \left(\frac{y^2}{r^2} - (1-2\nu_{\mathrm{u}}) \log r\right) H(t) + \frac{1}{\overline{\eta}}\left( \frac{(x^2-y^2)ct}{r^4}(1-\mathrm{e}^{-r^2/4ct}) + \tfrac{1}{4}E_1\left(\frac{r^2}{4ct}\right)\right)\right). \tag{C 11}$$

The stresses follow by differentiation and the constants in the potentials are given by

$$B_1 = -\pi b/2Gs|\chi|, \quad A_2 = -\pi b/2Gs\overline{\eta}(s/c), \tag{C 12}$$

$$A_1 + A_2 = -2(1-\nu_{\mathrm{u}})B_1/|\chi|. \tag{C 13}$$

### (b) *The opening dislocation with impermeable faces*

The constants in the potentials are given by

$$B_1 = -b\pi/2G\mathrm{i}\chi s, \quad A_2 = -\chi b\pi/\overline{\eta}(s/c)2G\mathrm{i}s\Gamma, \tag{C 14}$$

$$A_1|\chi| = -\Gamma A_2 - (1-2\nu_{\mathrm{u}})B_1. \tag{C 15}$$

### (c) *Point jump in pore pressure gradient*

Let us take an impulsively applied point jump in the pore pressure gradient on the $x$ axis

$$\left.\frac{\partial p}{\partial y}\right|_{y=0_+} - \left.\frac{\partial p}{\partial y}\right|_{y=0_-} = 2\pi q_0 \delta(x)H(t)2B(1+\nu_{\mathrm{u}})/3, \tag{C 16}$$

with continuity of stress and displacement across the x axis. From symmetry this is equivalent to taking $\sigma_{12} = u_2 = 0$ on $x = 0$. This is the solution required for the mixed problem in § 3. The constants in the potentials are given by

$$B_1 = 0, \quad \Gamma\overline{\eta}(s/c)A_2 = -|\chi|\overline{\eta}(s/c)A_1 = -\pi q_0/2Gs. \tag{C 17}$$

The field variables can be evaluated quite straightforwardly by using the inverse transform results in Appendix A.

## Appendix D. Near crack tip elastic eigensolutions

When using the reciprocal theorem we require the near crack tip fields for stress fields which are singular $O(r^{-1/2})$ and $O(r^{-3/2})$. Here we give the near notch tip fields for a notch of half angle $\beta$ loaded anti-symmetrically. The near crack tip fields are well known (for example, Sternberg & Koiter 1958) and are given here for completeness, they are deduced using the Mellin transform as in the similar tensile cases of Appendix D of [ACa]. The $\lambda$ below are the zeros of $\sin(2\lambda\beta) - \lambda \sin 2\beta$, and we consider notches which have $\beta^\star < \beta \leq \pi$, where $\beta^\star$ is the root of $\tan(2\beta) = 2\beta$. The $\overline{K}_{\mathrm{II}}(s)$ in the results below are the intensity factors, for the eigensolutions these $\overline{K}_{\mathrm{II}}(s)$ are written in the text as $\overline{K}^\star_{\mathrm{II}}(s)$ to distinguish them from the stress intensity factors. The results for a crack are recovered by taking $\beta = \pi$ and $\lambda = -1/2, 1/2$.

$$\overline{\sigma}_{rr}(r,\theta,s) = -\frac{\overline{K}_{\mathrm{II}}(s)}{2(2\pi)^{1/2}}((\lambda+3)\sin(\lambda+1)\theta \sin(\lambda-1)\beta - (\lambda-1)\sin(\lambda+1)\beta \sin(\lambda-1)\theta)r^{-\lambda-1}, \tag{D 1}$$

$$\bar{\sigma}_{r\theta}(r,\theta,s) = \frac{\overline{K}_{\mathrm{II}}(s)}{2(2\pi)^{1/2}}((\lambda+1)\sin(\lambda-1)\beta\cos(\lambda+1)\theta - (\lambda-1)\sin(\lambda+1)\beta\cos(\lambda-1)\beta)r^{-\lambda-1}, \tag{D 2}$$

$$\bar{\sigma}_{\theta\theta}(r,\theta,s) = \frac{(\lambda-1)\overline{K}_{\mathrm{II}}(s)}{2(2\pi)^{1/2}}(\sin(\lambda-1)\beta\sin(\lambda+1)\theta - \sin(\lambda+1)\beta\sin(\lambda-1)\theta)r^{-\lambda-1}, \tag{D 3}$$

$$\bar{u}_r(r,\theta,s) = \frac{\overline{K}_{\mathrm{II}}(s)}{4G\lambda(2\pi)^{1/2}}(\sin(\lambda-1)\beta\sin(\lambda+1)\theta((\lambda-1)+4(1-\nu)) - (\lambda-1)\sin(\lambda+1)\beta\sin(\lambda-1)\theta)r^{-\lambda}, \tag{D 4}$$

$$\bar{u}_\theta(r,\theta,s) = \frac{\overline{K}_{\mathrm{II}}(s)}{4G\lambda(2\pi)^{1/2}}((4(1-\nu)-(\lambda+1))\cos(\lambda+1)\theta\sin(\lambda-1)\beta + (\lambda-1)\sin(\lambda+1)\beta\cos(\lambda-1)\theta)r^{-\lambda}. \tag{D 5}$$

In the mixed anti-symmetric case the near crack tip pore pressure fields are given by

$$\bar{p}(r,\theta,s) = \overline{K}_3(s)(2\pi)^{-1/2}r^{(2n+1)\pi/2\beta}\sin((2n+1)\pi\theta/2\beta), \tag{D 6}$$

with $n$ taking integer values.

## References

Abramowitz, M. & Stegun, I. A. 1970 *Handbook of mathematical functions.* New York: Dover.

Atkinson, C. 1975 On the stress intensity factors associated with cracks interacting with an interface between two elastic media. *Int. J. Engng Sci.* **13**, 489–504.

Atkinson, C. 1991 Boundary elements and fracture stress analysis. *Engng Analysis Boundary Elements* **8**, 16–23.

Atkinson, C. & Craster, R. V. 1991 Plane strain fracture in poroelastic media. *Proc. R. Soc. Lond.* A**434**, 605–633.

Atkinson, C. & Craster, R. V. 1992*a* The application of invariant integrals in diffusive elastic solids. *Phil. Trans. R. Soc. Lond.* A**339**, 231–263.

Atkinson, C. & Craster, R. V. 1992*b* Some fracture problems in fully coupled dynamic thermoelasticity. *J. Mech. Phys. Solids* **40**, 1415–1432.

Atkinson, C. & Craster, R. V. 1993 A singular perturbation approach to integral equations occuring in poroelasticity. *IMA J. appl. Math.* (In the press.)

Atkinson, C. & Smelser, R. E. 1982 Invariant integrals of thermoviscoelasticity. *Int. J. Solids Structures* **18**, 533–549.

Auriault, J. L. 1980 Dynamic behaviour of a porous medium saturated by a Newtonian fluid. *Int. J. Engng Sci.* **18**, 775–785.

Biot, M. A. 1941 General theory of three-dimensional consolidation. *J. appl. Phys.* **12**, 155–164.

Biot, M. A. 1955 Thermoelasticity and irreversible thermodynamics. *J. appl. Mech.* **27**, 240–253.

Biot, M. A. 1956*a* The theory of propagation of elastic waves in a fluid saturated porous solid. I. The low frequency range. *J. acoust. Soc. Am.* **28**, 168–178.

Biot, M. A. 1956*b* The theory of propagation of elastic waves in a fluid saturated porous solid. II. The high frequency range. *J. acoust. Soc. Am.* **28**, 179–191.

Bowen, R. M. 1982 Compressible porous media models by use of the method of mixtures. *Int. J. Engng Sci.* **20**, 697–735.

Burridge, R. 1976 An influence function for the intensity function in tensile fracture. *Int. J. Engng Sci.* **14**, 725–734.





PHILOSOPHICAL TRANSACTIONS OF THE ROYAL SOCIETY A MATHEMATICAL, PHYSICAL & ENGINEERING SCIENCES

Burridge, R. & Keller, J. B. 1981 Poroelasticity equations derived from microstructure. *J. Acoust. Soc. Am.* **70**, 1140–1146.

Cleary, M. P. 1977 Fundamental solutions for a fluid saturated porous solid. *Int. J. Solids Struct.* **13**, 785–808.

Craster, R. V. & Atkinson, C. 1992*a* Shear cracks in thermoelastic and poroelastic media. *J. Mech. Phys. Solids* **40**, 887–924.

Craster, R. V. & Atkinson, C. 1992*b* Interfacial fracture in diffusive elastic media. *Int. J. Solids Struct.* **29**, 1463–1498.

Davies, B. & Martin, B. 1979 Numerical inversion of Laplace transforms: a survey and comparison of methods. *J. Comp. Phys* **33**, 1–32.

Detournay, E. & Cheng, A. H.-D. 1987 Poroelastic solution of a plane strain point displacement discontinuity. *ASME J. appl. Mech.* **54**, 783–787.

Eshelby, J. D. 1951 The force on an elastic singularity. *Phil. Trans. R. Soc. Lond.* A**244**, 87–112.

Piessens, R. 1975 A bibliography on numerical inversion of the Laplace transform and applications. *J. Comp. appl. Math.* **1**, 115–128. (Supplemented *J. Comp. appl. Math.* **2**, 225–228.)

Rice, J. R. 1972 Some remarks on elastic crack tip stress fields. *Int. J. Solids. Struct.* **8**, 751–758.

Rice, J. R. & Cleary, M. P. 1976 Some basic stress-diffusion solutions for fluid saturated elastic porous media with compressible constituents. *Rev. Geophys. Space Phys.* **14**, 227–241.

Rudnicki, J. W. 1985 Effect of pore fluid diffusion on deformation and failure of rock. In *Mechanics of geomaterials* (ed. Z. Bazant). John Wiley and Sons.

Rudnicki, J. W. 1987 Plane strain dislocations in linear elastic diffusive solids. *ASME J. appl. Mech* **54**, 545–551.

Skempton, A. 1954 The pore pressure coefficients *A* and *B*. *Geotechnique* **4**, 143–147.

Stehfest, H. 1970 Numerical inversion of Laplace transforms. *CACM* **13**, 47–49 and 624.

Sternberg, E. & Koiter, W. T. 1958 The wedge under a concentrated couple: a paradox in the two-dimensional theory of elasticity. *ASME J. appl. Mech.* **25**, 575–581.

Talbot, A. 1979 The accurate numerical inversion of Laplace transforms. *J. Inst. Math. Applic.* **23**, 97–120.

*Received 26 June 1992; accepted 5 February 1993*